bioRxiv preprint doi: https://doi.org/10.1101/245522; this version posted January 9, 2018. The copyright holder for this preprint (which was not certified by peer review) is the author/funder, who has granted bioRxiv a license to display the preprint in perpetuity. It is made available under a CC-BY 4.0 International license.

- 1 Septal Secretion of Protein A in Staphylococcus aureus
- 2 Requires SecA and Lipoteichoic Acid Synthesis
- 3
- 4 Wenqi Yu¹, Dominique Missiakas¹, Olaf Schneewind¹*
- 5 ¹Department of Microbiology, University of Chicago, Chicago, Illinois, USA

6

7 *For correspondence: oschnee@bsd.uchicago.edu

bioRxiv preprint doi: https://doi.org/10.1101/245522; this version posted January 9, 2018. The copyright holder for this preprint (which was not certified by peer review) is the author/funder, who has granted bioRxiv a license to display the preprint in perpetuity. It is made available under a CC-BY 4.0 International license.

9 Abstract

10	Surface proteins of Staphylococcus aureus are secreted across septal membranes for assembly
11	into the bacterial cross-wall. This localized secretion requires the YSIRK/GXXS motif signal
12	peptide, however the mechanisms supporting precursor trafficking are not known. We show
13	here that the signal peptide of staphylococcal protein A (SpA) is cleaved at the YSIRK/GXXS
14	motif. A signal peptide mutant defective for cleavage can be crosslinked to SecA, SecDF and
15	LtaS. SecA depletion blocks precursor targeting to septal membranes, whereas deletion of
16	secDF diminishes SpA secretion into the cross-wall. Depletion of LtaS blocks lipoteichoic acid
17	synthesis and promotes precursor trafficking to peripheral membranes. We propose a model
18	whereby SecA directs SpA precursors to lipoteichoic acid-rich septal membranes for YSIRK/GXXS
19	motif cleavage and secretion into the cross-wall.
20	
21	Introduction

22 Surface proteins of *Staphylococcus aureus* and other gram-positive cocci enter the secretory 23 pathway via their N-terminal signal peptides (Uhlén et al., 1984, DeDent et al., 2008). Once 24 translocated across the membrane, surface proteins are covalently linked to cell wall 25 peptidoglycan via sortase A-catalyzed cleavage at the LPXTG motif of C-terminal sorting signals (Schneewind et al., 1992, Schneewind et al., 1995, Mazmanian et al., 1999). Some, but not all 26 27 surface proteins are secreted at septal membranes and incorporated into cross-wall 28 peptidoglycan (Cole and Hahn, 1962, Carlsson et al., 2006, DeDent et al., 2008). Following 29 division and separation of spherical daughter cells, cross-wall anchored surface proteins are 30 displayed over large segments of the bacterial surface (DeDent et al., 2007). Cross-wall

31 trafficking of surface proteins requires a signal peptide with YSIRK/GXXS motif (Carlsson et al., 32 2006, DeDent et al., 2008). The YSIRK/GXXS motif is positioned N-terminal of the hydrophobic 33 core, common to all signal peptide precursors traveling the Sec pathway (Emr et al., 1978, Emr et al., 1981, von Heijne, 1986). 34 Gram-positive bacteria rely on cell wall-anchored surface proteins for adherence to host 35 36 tissues, evasion from host immune responses and acquisition of host-specific nutrients (Foster 37 et al., 2014). Surface proteins with YSIRK/GXXS signal peptides are produced with high 38 abundance and fulfill essential virulence functions during infection. For example, staphylococcal 39 protein A (SpA) is well known for its attribute of binding to host immunoglobulin and disrupting 40 adaptive immune responses (Forsgren and Siöquist, 1966, Kim et al., 2016), SpA is synthesized as a precursor with an N-terminal YSIRK/GXXS signal peptide and a C-terminal LPXTG motif 41 42 sorting signal (Abrahmsén et al., 1985, Schneewind et al., 1992). After initiation into the 43 secretion pathway, the signal peptide is cleaved by signal peptidase (Abrahmsén et al., 1985, 44 Schallenberger et al., 2012). Sortase A recognizes the LPXTG motif of the sorting signal, cleaves 45 the polypeptide between the threonine (T) and the glycine (G) of the LPXTG motif and forms an 46 acyl-enzyme intermediate with the C-terminal threonine (Mazmanian et al., 1999, Ton-That et 47 al., 1999). The acyl-enzyme is relieved by the nucleophilic attack of the amino-group of the 48 pentaglycine crossbridge within lipid II, the precursor for peptidoglycan synthesis (Ton-That et 49 al., 2000, Perry et al., 2002). The product of this reaction, surface protein linked to lipid II, is 50 then incorporated into peptidoglycan via the transglycosylation and transpeptidation reactions 51 of cell wall synthesis (Ton-That et al., 1997, Ton-That and Schneewind, 1999).

52	Newly synthesized SpA is secreted into the cross-wall compartment, bounded by septal					
53	membranes of burgeoning cells during division (DeDent et al., 2007). Upon completion of					
54	peptidoglycan synthesis within the cross-wall, its peptidoglycan layer is split (Frankel et al.,					
55	2011). The adjacent cells separate and assume a spherical shape, resulting in SpA display on the					
56	bacterial surface (DeDent et al., 2007). Staphylococci divide perpendicular to previous cell					
57	division planes (Tzagoloff and Novick, 1977). By incorporating secreted polypeptides into newly					
58	synthesized cross-walls, staphylococci distribute SpA and other sortase A-anchored products					
59	over the bacterial surface (DeDent et al., 2008). However, not all sortase-anchored products					
60	traffic to septal membranes. Those that are secreted at polar membranes are also anchored to					
61	peptidoglycan but are not distributed over the bacterial surface (DeDent et al., 2008). In S.					
62	aureus strain Newman, thirteen different sortase-anchored surface proteins and four additional					
63	proteins are endowed with YSIRK/GXXS signal peptides for septal secretion: lipase (Lip),					
64	glycerol-ester hydrolase (Geh), murein hydrolase LytN and the cell size determinant Ebh (Yu and					
65	Götz, 2012, Frankel et al., 2011, Cheng et al., 2014).					
66	The mechanisms supporting YSIRK/GXXS precursor secretion at septal membranes are					
67	not known. Here we show that the signal peptide of SpA is cleaved at the YSIRK/GXXS motif.					
68	Amino acid substitutions in the signal peptide that affect cleavage also impair SpA secretion.					
69	When used as a bait for the crosslinking of membrane proteins, purification of the SpA Ser ¹⁸ Leu					
70	(S18L) precursor identified SecA, SecDF and LtaS. We studied the contribution of these factors					
71	towards protein A secretion into the cross-wall compartment.					
72						

73 Results

bioRxiv preprint doi: https://doi.org/10.1101/245522; this version posted January 9, 2018. The copyright holder for this preprint (which was not certified by peer review) is the author/funder, who has granted bioRxiv a license to display the preprint in perpetuity. It is made available under aCC-BY 4.0 International license.

74 SpA signal peptide variants defective for septal secretion

75 To facilitate the analysis of signal peptide mutants, we generated SpA_{ED}, a variant of protein A 76 that is truncated for its C-terminal immunoglobulin binding domains, region X (Xr) and the 77 LPXTG sorting signal (Figure 1a). S. aureus WY110 ($\Delta spa \Delta sbi$, pSpA_{FD}) cultures expressing spa_{FD} 78 were fractionated into culture supernatant (S) and bacterial pellet (P) and analyzed by 79 immunoblotting. SpA_{FD} was found in the extracellular medium; its precursor species was 80 detected in the bacterial pellet (Figure 1bc). Site-directed mutagenesis was used to generate 81 short deletions and amino acid substitutions in the signal peptide of SpA_{ED} (Figure 1b). Deletion of the YISRK motif (Δ YSIRK) diminished the abundance of the SpA_{ED/ Δ YSIRK} precursor and its 82 83 processing (Figure 1b). Single amino acid substitutions at two positions in the YSIRK motif (I9S 84 and R10A) resulted in precursor accumulation (Figure 1b). Further, the R10A variant exhibited 85 diminished secretion and accumulated a precursor species that migrated faster on SDS-PAGE 86 than the full-length precursor (Figure 1bc). Amino acid substitution at lysine 11 (K11A) of the 87 YSIRK motif had no effect on SpA_{ED/K11A} precursor processing and secretion (Figure 1bc). 88 Deletion of GIAS (Δ GIAS) or of the two variable residues in the GXXS motif (Δ IA) caused 89 precursor accumulation and blocked precursor processing (Figure 1bc). Substitution of glycine 90 15 (G15L) reduced the abundance of SpA_{FD/G15L} and led to the accumulation of a unique 91 precursor species that migrated faster on SDS-PAGE than full-length precursor (*Figure 1b*). Substitution of serine 18 (S18L) caused accumulation of full-length and processed precursors as 92 93 well as reduced secretion (Figure 1bc). 94 S. aureus WY110 cultures were fractionated into culture supernatant (S), cell wall

95 extract (W), membranes (M) and cytoplasm (C). The SpA_{ED} precursor was found in the

96 cytoplasm and membrane, whereas mature product was secreted into the culture supernatant 97 (S) (*Figure 2a*). Precursors of the SpA_{ED/ $\Delta IA}$ and SpA_{ED/R10A} variants accumulated mostly in the</sub> 98 cytoplasm, whereas the SpA_{FD/S181} precursor was located predominantly in the membrane 99 (Figure 2ab). Pulse-labeling experiments revealed that wild-type SpA_{ED} precursor was processed 100 within 60 seconds into mature, secreted product (Figure 2c). In contrast, processing of the 101 SpA_{ED/AIA}, SpA_{ED/R10A} and SpA_{ED/S18L} precursors was delayed (*Figure 2c*). To test whether signal peptide variations affect trafficking of full-length SpA, mutations encoding the Δ IA, R10A and 102 103 S18L variants were introduced into wild-type *spa*. Wild-type and mutant staphylococci were 104 treated with trypsin to remove all surface proteins from the bacterial surface and incubated for 105 20 min to allow for cell wall deposition of newly synthesized SpA. To localize SpA, bacteria were 106 viewed by fluorescence microscopy after labeling with SpA-specific monoclonal antibody and 107 Alexa Fluor 647-conjugated secondary IgG (red) and with BODIPY FL-vancomycin (green), which 108 binds to cell wall peptidoglycan. As expected, wild-type SpA was assembled in the cross-wall 109 compartment, whereas SpA_{SP-SasF}, which is secreted via a canonical signal peptide, was 110 deposited into peripheral segments of the cell wall envelope (DeDent et al., 2008)(Figure 2d). 111 SpA_{ΔIA}, SpA_{R10A} and SpA_{S18L} exhibited defects in surface display, consistent with their observed 112 defects in precursor processing and secretion (Figure 2d). Residual amounts of cross-wall 113 localization were observed for SpA_{R10A} and SpA_{S18L}, whereas SpA_{ΔIA} was not detected in the 114 cross-wall compartment (Figure 2e). Together these data indicate that some features of the YSIRK/GXXS motif, specifically Arg¹⁰, Ser¹⁸ and the GXXS motif, are crucial for septal secretion of 115 116 SpA in S. aureus (Figure 2e).

bioRxiv preprint doi: https://doi.org/10.1101/245522; this version posted January 9, 2018. The copyright holder for this preprint (which was not certified by peer review) is the author/funder, who has granted bioRxiv a license to display the preprint in perpetuity. It is made available under a CC-BY 4.0 International license.

Processing of SpA signal peptide variants

119	Wild-type SpA _{ED} , SpA _{ED/ΔIA} , SpA _{ED/R10A} and SpA _{ED/S18L} were purified from staphylococcal
120	membranes via affinity chromatography, analyzed by Coomassie-stained SDS-PAGE and
121	identified by Edman degradation (<i>Figure 3a</i>). For wild-type SpA _{ED} , full-length precursor (SpA _{ED} -
122	1, starting at Met ¹), as well as two precursors with faster mobility on SDS-PAGE (SpA _{ED} -2 and
123	SpA _{ED} -3) and mature product (SpA _{ED} -4), i.e. SpsB signal peptidase-cleaved SpA _{ED} starting at
124	Ala ³⁷ , were identified (<i>Figure 3ab</i>). Edman degradation revealed that SpA _{ED} -2 is a product of
125	proteolytic cleavage within the YSIRK/GXXS motif (N-terminus Gly ¹³). SpA _{ED} -3 is a product of
126	further cleavage, as Edman degradation identified its N-terminal amino acid 10 residues
127	downstream (N-terminus Thr ²³) (<i>Figure 3ab</i>). Purified SpA _{ED} -1 precursor as well as its SpA _{ED} -2,
128	SpA _{ED} -3 and SpA _{ED} -4 cleavage products were analyzed by MALDI-TOF-MS, confirming the
129	predicted mass of the precursor and its cleaved species (Table 1). SDS-PAGE and Edman analysis
130	of the SpA _{ED/S18L} sample revealed the same four species as wild-type SpA _{ED} , albeit that the
131	abundance of SpA _{ED/S18L} -1 and SpA _{ED/S18L} -4 were increased over those of of SpA _{ED/S18L} -2 and
132	SpA _{ED/S18L} -3 (<i>Figure 3ab</i>). Analysis of the SpA _{ED/R10A} sample also identified four species, including
133	SpA _{ED/ R10A} -1 precursor, SpA _{ED/ R10A} -3 cleavage product (N-terminus Thr ²³) and SpA _{ED/ R10A} -4
134	mature product (N-terminus Ala 37), whereas SpA $_{\rm ED/R10A}$ -2 represented a variant cleavage
135	product (N-terminus Ala ¹⁰) (<i>Figure 3ab</i>). The SpA _{ED/ΔIA} sample yielded the same precursor and
136	cleavage species as SpA _{ED} and SpA _{ED/S18L} , however the abundance of SpA _{ED/ΔIA} -1 was increased
137	over that of SpA _{ED/<math>\Delta IA-2, SpAED/<math>\Delta IA-3 and SpAED/$\Delta IA-4 (Figure 3ab). Taken together, these data$</math></math>}
138	indicate that the SpA precursor (SpA _{ED} -1) is cleaved between Leu ¹² and Gly ¹³ , which are
139	positioned between the two motifs (underlined) of the <u>YSIRK</u> L/GV <u>GIAS</u> sequence. The R10A

substitution alters the cleavage site and diminishes precursor cleavage, whereas the S18L
substitution and ΔIA deletion diminish precursor cleavage without altering the cleavage site
between the YSIRK/GXXS motifs. Precursor cleavage between Gly²² and Thr²³ was observed for
all SpA variants, suggesting that it represents a proteolytic event unrelated to the function of
the YSIRK/GXXS motif in targeting SpA to septal membranes.

145

146 Identification of proteins cross-linked to a mutant SpA precursor

147 We used a biochemical approach to identify staphylococcal proteins that interact with SpA 148 precursor in septal membranes. The SpA_{S18L} precursor accumulates in septal membranes 149 (Figure 2bc), and SpA_{ED/S18L} precursor can be purified from these membranes (Figure 3ab). After 150 crosslinking with formaldehyde, SpA_{ED/S18L} precursor and associated species were isolated via 151 affinity chromatography, heat-treated to resolve crosslinks and analyzed by Coomassie-stained 152 SDS-PAGE and immunoblotting with anti-SpA (Figure 4ab). As compared to SpA_{FD/SP-SasF}, which 153 does not traffic to septal membranes and was not crosslinked to other proteins, several 154 proteins were specifically crosslinked to SpA_{ED/S181} and were identified by mass spectrometry 155 (Figure 4ab and Table S1). Most crosslinked proteins are components of the peptidoglycan 156 (PBP2, MurE2, MurG, FemA, FemB, FemX), wall teichoic acid (TagB, TagF) and lipoteichoic acid 157 synthesis pathways (LtaS) that are known to be localized to septal membranes (Pinho and 158 Errington, 2005, Mann et al., 2013, Reichmann et al., 2014). We also identified EzrA, a cell 159 division machinery component (Steele et al., 2011). SecA and SecDF, members of the bacterial 160 protein secretory pathway (Oliver and Beckwith, 1981, Gardel et al., 1987, Pogliano and Beckwith, 1994), and LtaS, lipoteichoic acid synthase (Gründling and Schneewind, 2007), were 161

162 selected for further study. Immunoblotting confirmed SecA crosslinking to the SpA_{ED/S18L}

163 precursor (*Figure 4c*).

164

165 SecA depletion in S. aureus

166 In *Escherichia coli, secA* is an essential gene (Oliver and Beckwith, 1981). SecA functions as an

167 ATPase that moves many, but not all, precursor proteins across the SecYEG translocon

168 (Tsirigotaki et al., 2017). To study the contribution of *secA* towards the septal secretion of SpA,

169 we generated an inducible allele, P_{spac}-secA, in S. aureus WY223 (Figure 5a). When induced with

170 isopropyl β-D-1-thiogalactoside (IPTG), *S. aureus* WY223 (P_{spac}-secA) forms colonies on agar and

171 replicates in liquid media culture in a manner similar to wild-type *S. aureus* (*Figure 5bc*).

However, in the absence of IPTG, *S. aureus* WY223 cannot form colonies or replicate in broth

173 culture (*Figure 5bc*). Following dilution of bacteria from IPTG-containing media into broth

174 without inducer, S. aureus WY223 replicates for 3 hours at a rate similar to wild-type (Figure

175 5b). Upon further dilution and incubation, S. aureus WY223 eventually exhibits growth

176 retardation and arrest (6-hour time point). When analyzed by immunoblotting with SecA-

177 specific antibody, SecA was depleted in *S. aureus* WY223 (P_{spac}-secA) cultures 3 hours following

dilution into inducer free medium. After 6 hours of incubation, SecA could no longer be

179 detected (*Figure 5d*).

180

181 SecA depletion blocks SpA secretion

182 After dilution into media with and without inducer, wild-type (S. aureus RN4220) and P_{spac}-secA

183 (*S. aureus* WY223) were subjected to pulse labeling with [³⁵S]methionine and protein A

184 precursor processing was analyzed by immunoprecipitation. In wild-type, SpA precursors are 185 processed within 60 seconds; similar rates of processing were observed when the P_{spac}-secA 186 mutant was grown with IPTG inducer (Figure 6a). In the absence of IPTG, SpA precursor processing was slowed to about 5 min, indicating that SecA depletion inhibits precursor 187 188 translocation (Figure 6a). When analyzed by fluorescence microcopy in trypsin-treated 189 staphylococci incubated for 20 min without protease, wild-type S. aureus deposited protein A 190 into the cross wall (Figure 6b, yellow arrow). Cross wall localization was diminished in P_{spac}-secA 191 mutant bacteria grown without IPTG inducer and restored to wild-type levels when bacteria 192 were grown in the presence of inducer (*Figure 6c*). Six hours after dilution into broth without 193 IPTG inducer, S. aureus WY223 (P_{spac}-secA) cells were grossly enlarged and surrounded by a thin layer of peptidoglycan with aberrant cross-wall formation (Figure 6d, blue arrow); at this time 194 195 point, SpA could not be detected in the bacterial envelope. As a control, growth of S. aureus 196 WY223 in the presence of IPTG did not affect cell size and SpA deposition into the cell wall 197 (Figure 6d).

198 We wondered whether SecA depletion affects the secretion of other staphylococcal 199 proteins. Glycerol-ester hydrolase (Geh) is synthesized as a precursor with YSIRK/GXXS signal 200 peptide motif (Lee and Iandolo, 1986). Following secretion at septal membranes into the cross-201 wall compartment, Geh is subsequently released into the extracellular medium (Yu and Götz, 202 2012). When analyzed by immunoblotting of proteins in the extracellular medium, depletion of 203 SecA in S. aureus WY223 (Pspac-secA) caused a reduction in secreted Geh, as compared to wild-204 type staphylococci or S. aureus WY223 grown in the presence of IPTG (Figure 6e). Staphylooccal 205 nuclease (Nuc), a secreted protein that contribute to the pathogenesis of human and animal

infections, is synthesized as a precursor with a canonical signal peptide (Phonimdaeng et al.,
1990, Shortle, 1983). The abundance of secreted Nuc was also diminished in SecA-depleted
cultures of *S. aureus* WY223 (*Figure 6e*). As a control, production of sortase A in staphylococcal
membranes was not affected by the depletion of SecA. Taken together, these data indicate that
SecA is essential for *S. aureus* growth and for the secretion of precursors with canonical and
YSIRK/GXXS signal peptides.

212

213 Localization of SecA and SpA precursors in staphylococci

To localize SecA within *S. aureus*, we generated a translational hybrid between *secA* and the

structural gene for super-folder green fluorescent protein (*gfp*) (Pedelacq et al., 2006) under

transcriptional control of the P_{tet} promoter in S. aureus WY230 (P_{spac}-secA, P_{tet}-secA:sfGFP,

217 *Figure 7a*). Expression of *secA:sfGFP* in the P_{spac}-secA variant restored bacterial growth in the

absence of IPTG inducer, indicating that *secA-gfp* is functional (*Figure 7b*). Growth restoration

219 occurred in the presence and in the absence of anhydrotetracycline (ATc), suggesting that

secA:sfGFP must be expressed even in the absence of the P_{tet} inducer (*Figure 7b*).

221 Immunoblotting staphylococcal cell extracts 3 and 6 hours following dilution into media lacking

222 IPTG revealed that S. aureus WY230 indeed produced small amounts SecA:sfGFP in the absence

of ATc (*Figure 7c*). In the presence of ATc inducer, the abundance of SecA-GFP was increased

224 (Figure 7c). As expected, wild-type SecA was depleted when S. aureus WY230 was cultured for 3

or 6 hours without the IPTG inducer (*Figure 7b*). However, under SecA depleting conditions,

even small amounts of SecA-sfGFP in S. aureus WY230 (-ATc) restored precursor processing of

227 pulse-labeled SpA (*Figure 7d*). SpA precursor processing was accelerated to levels faster than

228 wild-type when *S. aureus* WY230 cultures were grown in the presence of ATc (*Figure 7d*). 229 Fluorescence microscopy of S. aureus WY230 stained with the membrane dye FM4-64 (red) 230 revealed SecA-sfGFP localization to plasma membranes (Figure 7e). In dividing cells, SecA-sfGFP 231 was found on septal (yellow arrow) and on polar membranes (orange arrow, Figure 7e). ATc-232 induced overexpression of SecA-sfGFP caused accumulation of hybrid protein throughout the 233 cytoplasm (Figure 7e). Thus, in S. aureus WY230, SecA-sfGFP is associated throughout the 234 plasma membranes and not restricted to the septal membrane. 235 The envelope of trypsin-treated, paraformaldehyde-fixed S. aureus WY223 (P_{spac} -secA) 236 was permeabilized with murein hydrolase and with detergent to detect intracellular precursors 237 via microscopy with fluorescent antibody (Harry et al., 1995, Pinho and Errington, 2003). In S. 238 aureus WY223 producing wild-type levels of SecA (P_{spac}-secA + IPTG), SpA precursors were 239 localized to septal membranes (Figure 8a). In other images, SpA precursors appeared as two 240 puncta or ring deposits at septal membranes, reminiscent of FtsZ and of the division rings that 241 are known to accumulate at this site (Figure 8ab)(Lutkenhaus, 1993). In contrast, under SecA 242 depleting conditions (-IPTG), SpA precursors in S. aureus WY223 were associated with polar 243 membranes and were not localized to septal membranes (Figure 8a). These results suggest that 244 in staphylococci with a functional secretion pathway, SpA precursor are localized to the vicinity 245 of septal division rings. However, in cells lacking functional secretion machines, SpA precursors 246 are located throughout the cytoplasm and cannot traffic to septal membranes. 247

248 SecDF contributes to SpA secretion

249 The secDF gene is not essential for protein secretion and S. aureus growth, however secDF 250 mutants exhibit diminished secretion of many precursors secreted via canonical and YSIRK-251 GXXS signal peptides (Quiblier et al., 2011, Quiblier et al., 2013). SecDF is a member of the 252 resistance nodulation and cell division (RND) membrane protein family with 12-transmembrane 253 spanning segments. SecDF functions as a membrane-integrated chaperone. Sustained by the 254 proton motive force, SecDF catalyzes ATP-independent translocation and folding of proteins on 255 the trans-side of the plasma membrane (Tsukazaki et al., 2011). S. aureus expresses two 256 additional RND proteins, here designated Rnd2 (SAOUHSC 02525) and Rnd3 (SAOUHSC 02866) 257 (Quiblier et al., 2011). The rnd2 gene is located downstream of femX, whose product tethers 258 glycine from glycyl-tRNA to the ε -amino group of lysine in lipid II peptidoglycan precursor [C₅₅-259 (PO₄)₂-MurNAc(L-Ala-D-iGln-L-Lys-Da-Ala-D-Ala)-GlcNac](Rohrer et al., 1999). Rnd2 product 260 interacts with FemB, PBP1 and PBP2 (Quiblier et al., 2011). As SecDF, FemB and PBP2 were each 261 found crosslinked to SpA_{ED/S18L} precursors (*Table S1*), we asked whether secDF, rnd2 and rnd3 262 contribute to septal secretion of SpA. Compared to wild-type S. aureus, the \triangle secDF mutant (S. 263 aureus WY418) accumulated SpA_{FD} precursor in bacterial cells and secreted reduced amounts 264 of mature SpA_{ED} into the extracellular medium (Figure 9ab). S. aureus rnd2 (WY416) and rnd3 265 (WY400) mutants exhibited wild-type levels of SpA_{ED} secretion (*Figure 9ab*). A variant lacking all 266 three genes, $\Delta secDF \Delta rnd23$, accumulated precursors at a level similar to the $\Delta secDF$ mutant 267 (*Figure 9ab*). When analyzed for other secreted proteins, the \triangle secDF mutant secreted 268 diminished amounts of Geh and failed to secrete Coa, whose precursor is secreted via a 269 canonical signal peptide (Phonimdaeng et al., 1990), while the $\Delta rnd2$ and $\Delta rnd3$ variants 270 displayed wild-type phenotypes (Figure 9ab). Thus, SecDF, but not Rnd2 and Rnd3, contributes

271	to protein secretion in S. aureus. Immunofluorescence microscopy experiments revealed that						
272	septal secretion of SpA was diminished in the $\Delta secDF$ and $\Delta secDF \Delta rnd23$ mutants (<i>Figure 9c</i>).						
273	Unlike SecA-depleted cells, where SpA precursors failed to associate with septal membranes,						
274	Δ secDF and Δ secDF Δ rnd23 mutants exhibited puncta of SpA precursors and rings of low						
275	fluorescent intensity at septal membranes (Figure 9c). The diminished abundance of SpA						
276	precursors at septal membranes was restored to wild-type levels by plasmid-borne expression						
277	of <i>secDF</i> in Δ <i>secDF</i> (pSecDF) and in Δ <i>secDF</i> Δ <i>rnd23</i> (pSecDF) staphylococci (<i>Figure 9c</i>). These						
278	data suggest that SecDF aids in the translocation of SpA across staphylococcal membranes but						
279	is not required precursor targeting to septal membranes.						
280							
281	LtaS is required for septal localization of SpA						
282	LtaS-mediated synthesis of lipoteichoic acid, a polyglycerol-phosphate polymer decorated with						
282 283	LtaS-mediated synthesis of lipoteichoic acid, a polyglycerol-phosphate polymer decorated with esterified D-alanyl and GlcNAc residues, is essential for <i>S. aureus</i> growth and cell division						
283	esterified D-alanyl and GlcNAc residues, is essential for <i>S. aureus</i> growth and cell division						
283 284	esterified D-alanyl and GlcNAc residues, is essential for <i>S. aureus</i> growth and cell division (Gründling and Schneewind, 2007). Earlier work generated <i>S. aureus</i> P _{spac} -ItaS, a strain with						
283 284 285	esterified D-alanyl and GlcNAc residues, is essential for <i>S. aureus</i> growth and cell division (Gründling and Schneewind, 2007). Earlier work generated <i>S. aureus</i> P _{spac} - <i>ItaS</i> , a strain with IPTG-inducible expression of lipoteichoic acid synthase. In the absence of IPTG inducer, LtaS is						
283 284 285 286	esterified D-alanyl and GlcNAc residues, is essential for <i>S. aureus</i> growth and cell division (Gründling and Schneewind, 2007). Earlier work generated <i>S. aureus</i> P _{spac} - <i>ItaS</i> , a strain with IPTG-inducible expression of lipoteichoic acid synthase. In the absence of IPTG inducer, LtaS is depleted in <i>S. aureus</i> ANG499 (P _{spac} - <i>ItaS</i>), providing an experimental system to study the effects						
283 284 285 286 287	esterified D-alanyl and GlcNAc residues, is essential for <i>S. aureus</i> growth and cell division (Gründling and Schneewind, 2007). Earlier work generated <i>S. aureus</i> P _{spac} - <i>ItaS</i> , a strain with IPTG-inducible expression of lipoteichoic acid synthase. In the absence of IPTG inducer, LtaS is depleted in <i>S. aureus</i> ANG499 (P _{spac} - <i>ItaS</i>), providing an experimental system to study the effects of LTA synthesis on septal secretion of SpA (Gründling and Schneewind, 2007). Surface proteins						
283 284 285 286 287 288	esterified D-alanyl and GlcNAc residues, is essential for <i>S. aureus</i> growth and cell division (Gründling and Schneewind, 2007). Earlier work generated <i>S. aureus</i> P _{spac} - <i>ItaS</i> , a strain with IPTG-inducible expression of lipoteichoic acid synthase. In the absence of IPTG inducer, LtaS is depleted in <i>S. aureus</i> ANG499 (P _{spac} - <i>ItaS</i>), providing an experimental system to study the effects of LTA synthesis on septal secretion of SpA (Gründling and Schneewind, 2007). Surface proteins were removed with trypsin and staphylococci were incubated for 20 min to localize deposition						
283 284 285 286 287 288 288 289	esterified D-alanyl and GlcNAc residues, is essential for <i>S. aureus</i> growth and cell division (Gründling and Schneewind, 2007). Earlier work generated <i>S. aureus</i> P _{spac} - <i>ItaS</i> , a strain with IPTG-inducible expression of lipoteichoic acid synthase. In the absence of IPTG inducer, LtaS is depleted in <i>S. aureus</i> ANG499 (P _{spac} - <i>ItaS</i>), providing an experimental system to study the effects of LTA synthesis on septal secretion of SpA (Gründling and Schneewind, 2007). Surface proteins were removed with trypsin and staphylococci were incubated for 20 min to localize deposition of newly synthesized SpA (<i>Figure 10bc</i>). LtaS depletion (-IPTG) resulted in SpA deposition into						

293	lysostaphin- and detergent-permeabilized staphylococci revealed SpA targeting to septal
294	membranes in wild-type (S. aureus RN4220) and in IPTG-induced S. aureus ANG499 (P _{spac} -
295	<i>ltaS</i>)(<i>Figure 10d</i>). In contrast, without IPTG inducer, <i>S. aureus</i> ANG499 mislocalized SpA
296	precursors to polar membranes (Figure 10d). Protein secretion and cell wall anchoring of SpA
297	were analyzed by immunoblotting in <i>S. aureus</i> cultures separated into culture supernatant (S)
298	and bacterial sediment (P, pellet) samples. These experiments revealed that LtaS depletion in S.
299	aureus ANG499 (P _{spac} -ItaS, -IPTG) diminished the abundance of cell wall anchored SpA without
300	affecting the secretion of Geh and Nuc (<i>Figure 10e</i>). Consistent with the immunoblotting
301	results, LtaS depletion diminished the overall surface distribution of SpA (Figure 10f), in
302	agreement with the hypothesis that cross-wall targeting via the YSIRK/GXXS signal peptide, but
303	not polar secretion, is responsible for efficient surface distribution of proteins in staphylococci
304	(Carlsson et al., 2006, DeDent et al., 2008). Together these data indicate that LtaS depletion
305	and a block in lipoteichoic acid synthesis abolished SpA precursor trafficking to septal
306	membranes without affecting its secretion at polar membranes.
307	
308	Discussion
309	Cell wall-anchored surface proteins with YSIRK/GXXS motif signal peptides have been identified
310	in streptococcal and staphylococcal species (Tettelin et al., 2005, Rosenstein and Götz, 2000).
311	Although sortase-anchored surface proteins are found in many different gram-positive bacteria,
312	the signal peptides of surface proteins in rod-shaped bacteria of the genus Actinomyces,

313 Bacillus, Clostridium, and Listeria do not contain the YSIRK/GXXS motif. Common features of

314 staphylococci and streptococci are their spherical or ovoid cell shapes and cell wall synthesis

315	programs at septal membranes; in staphylococci this compartment is designated as the cross-
316	wall (Giesbrecht et al., 1976, Touhami et al., 2004, Monteiro et al., 2015). Earlier work
317	demonstrated that the YSIRK/GXXS motif of the SpA precursor is dispensable for sortase-
318	catalyzed cell wall anchoring (Bae and Schneewind, 2003). However, precursors with
319	YSIRK/GXXS motif signal peptides are targeted for secretion at septal membranes and sortase-
320	mediated deposition into the cross wall compartment (Carlsson et al., 2006, DeDent et al.,
321	2008). After completion of cross-wall synthesis, peptidoglycan splitting and cell separation, the
322	anchored products of <i>spa</i> and of other genes with YSIRK/GXXS motif signal peptides are
323	distributed over the bacterial surface (Cole and Hahn, 1962, DeDent et al., 2007). In contrast,
324	surface proteins with canonical signal peptides are deposited by sortase into polar
325	peptidoglycan but cannot be distributed over bacterial surfaces (Carlsson et al., 2006, DeDent
326	et al., 2008).

Although it is clear that YSIRK/GXXS signal peptides are necessary and sufficient for 327 328 septal secretion of proteins, the mechanisms supporting such trafficking were heretofore not known. We show that the YSIRK/GXXS signal peptide of SpA is cleaved between Leu¹¹ and Gly¹², 329 330 separating the YSIRK sequence from the GXXS motif and from the remainder of the signal 331 peptide. Amino acid substitutions and deletions that affect precursor cleavage and secretion 332 map to three of the four residues (underlined) that are strictly conserved in the YSIRK/GXXS motif: Ile⁹, Arg¹⁰ and Ser¹⁸. Substitution of the fourth residue, Gly¹⁵, with Leu resulted in 333 334 diminished abundance of precursor substrate and secreted product and in accumulation of a 335 cleaved precursor species (Figure 1b). On the basis of these observations, we are compelled to 336 speculate that YSIRK/GXXS motif cleavage may represent a mechanism for precursor

337 translocation at septal membranes. For example, the YSIRK/GXXS motif may inhibit a key 338 function of the adjacent hydrophobic core within signal peptides: promoting the membrane 339 translocation of precursors. Such inhibitory mechanism could be relieved by a YSIRK/GXXS 340 protease that localizes to the septal membrane. Other mechanisms of proteolytic control for 341 YSIRK/GXXS mediated signal peptide function can also be thought of. Importantly, the discovery 342 of two sequential proteolytic events, YSIRK/GXXS motif cleavage and the signal peptidase-343 mediated cut provide new experimental opportunities for the testing of predictive models. SpA precursors were also cut between Gly²² and Thr²³, a site that is located within the hydrophobic 344 345 core of the signal peptide. Mass spectrometry analysis of the S. aureus COL secretome also 346 identified signal peptide fragments that had been generated by cleavage in the hydrophobic core, including SpA signal peptides cleaved between Gly²² and Thr²³ (Ravipaty and Reilly, 2010). 347 348 The significance of signal peptide cleavage in the hydrophobic core is not known, as amino acid 349 substitutions preventing such proteolysis have not be studied for their effect on protein secretion or membrane integrity. We presume that cleavage at Gly^{22}/Thr^{23} may not be related 350 351 to septal secretion. Cleavage at the hydrophobic core may enable staphylococci to remove the 352 products of processed signal peptides from the membrane. For example, products of 353 degradative proteolysis have been observed during processing of SpA LPXTG motif sorting 354 signal, which is cleaved between Thr (T) and Gly (G) and within the hydrophobic core (Navarre 355 and Schneewind, 1994).

Precursors with amino acid substitutions or deletions in the YSIRK/GXXS motif are
thought to accumulate in septal membranes, however these variants typically exhibit
diminished secretion and cell wall anchoring in the cross wall (DeDent et al., 2008, Yu and Götz,

359 2012). Our observations corroborate these findings and suggest that not all features of the 360 YSIRK/GXXS motif are required for precursor targeting to septal membranes. We took 361 advantage of the SpA_{FD/S181} precursor and used affinity chromatography to purify crosslinked 362 proteins. Several crosslinked proteins were already known to be located in septal membranes 363 (PBP2, EzrA, LtaS), consistent with SpA_{ED/S18L} precursor accumulation in this compartment. 364 Among the crosslinked proteins are two components of the secretion machinery, SecA and 365 SecDF, as well as LtaS, which catalyzes the synthesis of lipoteichoic acid in septal membranes 366 (Tsirigotaki et al., 2017, Percy and Gründling, 2014). 367 The subcellular localization of the Sec apparatus has been examined in streptococci, 368 enterococci and in Bacillus subtilis. A spiral pattern of Sec translocase has been reported for B. 369 subtilis (Campo et al., 2004). In S. pyogenes, contradictory results have been reported for 370 immunogold-labelling and electron microscopy experiments: SecA was localized to a single 371 microdomain and also found distributed throughout the plasma membrane (Carlsson et al., 372 2006, Rosch and Caparon, 2004). In S. pneumoniae, SecA localization changed during cell cycle 373 progression. In early divisional cells, SecA was predominantly localized to septal membranes, 374 whereas during later stages of division SecA was hemispherically distributed within the region 375 between septa and at the future equators of dividing cells (Tsui et al., 2011). Streptococcus 376 agalactiae SecA was localized to septal membranes, whereas SecA was detected as a single 377 microdomain in Streptococcus mutans and Enterococcus faecalis (Brega et al., 2013, Hu et al., 378 2008, Kline et al., 2009). We show here that S. aureus SecA is localized to the plasma 379 membrane and is not spatially restricted to septal membranes or microdomains. This

distribution is consistent with our proposed role of SecA, promoting precursor translocation at
 polar and septal membranes.

382 When studied for its contribution to septal secretion, SecDF chaperone allows large 383 amounts of protein A to be deposited into the cross-wall peptidoglycan and promotes secretion 384 of YSIRK/GXXS motif precursors (SpA and Geh). Nevertheless, secDF is not essential for septal 385 targeting or secretion of SpA precursors. In contrast, cells depleted for SecA, accumulate SpA 386 precursors that cannot traffic to septal membranes in the cytoplasm. Finally, LtaS-depleted 387 staphylococci are unable to synthesize lipoteichoic acid and cannot direct precursors to the 388 septal area; instead, SpA is directed to polar membranes. We have incorporated these 389 observations into a model whereby septal accumulation of LtaS and of lipoteichoic acids 390 functions as a determinant for SecA-mediated targeting of SpA precursors. Following precursor 391 cleavage at the YSIRK/GXXS motif, truncated SpA (SpA-2) is moved across the membrane, aided 392 by the proton-motif force and by the chaperone activity of SecDF. Once translocated, SpA is 393 cleaved by signal peptidase to generate SpA-4 and by sortase at the LPXTG motif of its C-394 terminal sorting signal (Navarre and Schneewind, 1994, Ton-That et al., 1999). The resulting 395 sortase-acyl intermediate is then incorporated into cross wall peptidoglycan for distribution on 396 the bacterial surface (Schneewind et al., 1995).

397

398 Materials and methods

Bacterial strains and growth conditions

400 *E. coli* strains were grown in Luria-Bertani broth (LB) or LB agar. *S. aureus* strains were grown in

401 tryptic soy broth (TSB) or tryptic soy agar (TSA). Ampicillin (100 μg/ml) was used for plasmid

402	selection in <i>E. coli</i> . Chloramphenicol was used for selection of pOS1 derivatives (10 μ g/ml) and
403	pCL55 derivatives (5 μ g/ml) in <i>S. aureus</i> (Lee et al., 1991). Erythromycin (Erm 10 μ g/ml) was
404	used for selection of <i>ermB</i> marked <i>bursa aurealis</i> transposon mutants in <i>S. aureus</i> WY110 (Δ <i>spa</i>
405	Δsbi) and 10 µg/ml Erm plus 1 mM isopropyl eta -D-1-thiogalactopyranoside (IPTG) was used for
406	pMutin–HA-5'secA selection in <i>S. aureus</i> . Protein expression from Pspac promoter was induced
407	with 1 mM IPTG. Anydrotetracycline (ATc, 200 ng/ml) was used to induce expression from the
408	tetracycline-inducible promoter in pCL55-P _{tet} constructs.

410 Plasmids and strains

411 To avoid mutations in the spa gene, all cloning procedures were performed at 30°C. All the 412 pOS1-derivative and pCL55-derivative plasmids were constructed in *E. coli* DC10B (Monk et al., 413 2012) and transformed to S. aureus strains by electroporation (Schneewind and Missiakas, 414 2014). All the plasmids or strains constructed were confirmed by sequencing (Table S2). Primers 415 used in this study are listed in Table S3. To avoid cross reaction in SpA immunoblot and 416 purification, S. aureus WY110 (Δspa Δsbi) was generated by transducing the sbi::ermB allele 417 from the Phoenix library (Bae et al., 2004) into S. aureus SEJ1, i.e. S. aureus RN4220 carrying 418 Δspa . Phage transduction was performed as described previously (Schneewind and Missiakas, 419 2014). To construct pSpA_{ED}, primers 10 and 69 were used to amplify the spa promoter and 420 spa_{FD} coding sequence encoding IgBDs E and D (-40 bp upstream of the transcription start site 421 of spa to 459 bp of spa coding sequence) from chromosomal DNA of S. aureus RN4220. The PCR 422 product was digested with EcoRI and BamHI, and ligated with plasmid pOS1 (Schneewind et al., 423 1993). To generate mutations and deletions within SpA signal peptide sequence, quick-change

424 mutagenesis was performed as follows: primers pairs (Table S3) that contain desired mutation 425 or deletion were used to PCR amplify pSpA_{ED}. The PCR products were digested with DpnI and 426 transformed to E. coli DC10B. Plasmid variants confirmed by DNA sequencing were transformed 427 to S. aureus WY110. To construct pCL55-SpA and its derivatives, primer pairs 175 and 177 were 428 used to PCR amplify the spa promoter and full-length spa coding sequence. PCR products were 429 digested with BamHI and KpnI and ligated into pCL55 cut with the same enzymes (Lee et al., 430 1991). The resulting plasmid pCL55-SpA was used as template for PCR mutagenesis of its signal 431 peptide mutant derivatives via quick-change mutagenesis as described above. To construct 432 pCL55-SpA_{SP-SasF}, primer pairs 175 and 21 were used to amplify the promoter sequence of *spa*. 433 Primers 22 and 23 were used to amplify coding sequence for the signal peptide sequence of 434 sasF. Last, primers 24 and 177 were used amplify spa coding sequence for the E and D IgBDs. All 435 three DNA fragments were ligated via SOE (splicing by overlap extension) PCR, digested with 436 BamHI and KpnI, and then ligated into pCL55 cut with the same restriction enzymes. pCL55-437 derivaties were transformed to S. aureus WY110 and integrated into the chromosome at the 438 *geh* locus (Lee et al., 1991). The integration was confirmed by PCR. To construct the *secA* 439 depletion strain S. aureus WY223 (P_{snac}-secA), primers 189 and 190 were used to amplify the 440 ribosome binding site and the first 656 bp of the secA gene. The PCR product was digested with 441 HindIII and KpnI and ligated with pMutin–HA (Bacillus Genetic Stock Center, Columbus, OH). 442 The resulting plasmid pMutin–HA-5'secA was transformed into RN4220 and integrated at the 443 secA locus in the chromosome. Clones were selected on TSA supplemented with 10 μ g/ml 444 erythromycin and 1 mM IPTG. To construct pCL55-P_{tet}-secA:sfGFP, primers 180 and 181 were 445 used to amplify *secA* full-length coding sequence together with its ribosome binding site.

446 Primers 182 and 183 were used to amplify sfGFP gene from pCX-sfGFP (Yu and Götz, 2012). The 447 two DNA fragments were joined together by SOE. The resulting *secA:sfGFP* hybrid, which 448 contains the 'Gly-Gly-Ala-Ala-Gly-Ala' between SecA and sfGFP, was digested with AvrII-BgIII 449 and ligated with pCL55-P_{tet} (Gründling and Schneewind, 2007). pCL55-P_{tet}-secA:sfGFP was 450 transformed to into S. aureus WY223 (P_{spac}-secA) and integrated into the chromosome at the 451 geh locus, thereby generating S. aureus WY230 (Pspac-secA, Ptet-secA:sfGFP). Plasmid pKOR1 452 based allelic replacement strategy (Bae and Schneewind, 2006) was used to generate the 453 ΔsecDF (S. aureus WY418) and Δrnd2 (S. aureus WY416) knock-out mutants. S. aureus WY412, a 454 mutant with $\Delta secDF \Delta rnd23$ mutations, was generated by transducing the rnd3::ermB allele 455 from the Phoenix library into S. aureus carrying $\Delta secDF$ and $\Delta rnd2$ mutations. To construct the 456 complementation plasmid pSecDF, the secDF ORF and 274 bp upstream sequence were PCR 457 amplified with primers 315 and 316, digested with EcoRI and BamHI, and ligated into pOS1 cut 458 with the same enzymes. The resulting plasmid, pSecDF, was transformed into S. aureus strains 459 WY418 (Δ secDF) and WY412 (Δ secDF Δ rnd23).

460

461 Cell fractionation and immunoblotting

Bacterial overnight cultures were diluted 1: 100 into fresh TSB and grown to OD_{600} 0.8. One ml culture was centrifuged at 18,000 ×*g* for 5 min in an Eppendorf tube. The culture supernatant (S) was transferred to another tube and proteins were precipitated with 10 % trichloroacetic acid (TCA) on ice for 30 min. The bacterial sediment (P, pellet) was suspended in 1 ml Trisbuffer [50 mM Tris-HCl (pH 7.5), 150 mM NaCl]and incubated with 20 µg/ml lysostaphin at 37°C for 30 min. After cell lysis, proteins from the cell pellet were precipitated with 10% TCA. To

468	localize proteins in different cellular compartments, cell fractionation was performed as						
469	follows: 1 ml culture (OD ₆₀₀ =0.8) was centrifuged at 18,000 $\times g$ for 5 min in an Eppendorf tube.						
470	The supernatant was transferred to a new tube and proteins were precipitated with 10% TCA						
471	(S, supernatant). The pellet was suspended in 1 ml TSM [50 mM Tris-HCl (pH 7.5), 0.5 M						
472	sucrose, 10 mM MgCl_2] and incubated with 20 μ g/ml lysostaphin for 10 min at 37°C. After						
473	centrifugation at 18,000 $ imes g$ for 5 min, the supernatant (cell wall fraction) was transferred to						
474	another tube. The protoplast pellet was suspended in 1 ml Tris-buffer and subjected to freeze-						
475	thaw cycle for 3 times in dry ice/ethanol bath and warm water. Membranes were in the cell						
476	lysate were sedimented by ultracentrifugation 150,000 $ imes g$ for 40 min. Supernatant was						
477	transferred to another tube (cytosolic fraction) whereas the pellet (membrane fraction) was						
478	suspended in 1 ml Tris-buffer and precipitated with 10% TCA. After TCA precipitation on ice for						
479	30 min, proteins were sedimented at 18,000 $ imes g$ for 10 min, washed with ice-cold acetone, air-						
480	dried and solubilized in 100 μ l 1×SDS sample buffer [62.5 mM Tris-HCl (pH 6.8), 2 % SDS, 10 %						
481	glycerol, 5 % 2-mercaptoethanol, 0.01 % bromophenol blue]. For immunoblotting, protein						
482	samples were separated on 10%, 12% or 15% SDS-PAGE and transferred to polyvinylidene						
483	difluoride (PVDF) membranes. Membranes were blocked with 5% milk for 45 min. As needed,						
484	50 μ l human IgG (Sigma) was added to 10 ml block-solution to block SpA cross-reaction. Primary						
485	antibodies were affinity-purified rabbit polyclonal antibodies against SpA _{KKAA} (1:10,000						
486	dilution), rabbit serum of anti-SrtA (1:20,000 dilution), rabbit serum of anti-SecA (1:10,000						
487	dilution), rabbit serum of anti-Geh (1:10,000 dilution), polyclonal antibodies of anti-Coa						
488	(1:5,000 dilution), rabbit serum of anti-Nuc (1:5,000 dilution), and anti-GFP rabbit serum						
489	(1:10,000 dilution) (Invitrogen). Membranes were incubated with primary antibodies for 1 h,						

490	washed three times for 5 min with TBST [50 mM Tris(pH 7.5), 150 mM NaCl, 0.1% Tween 20],
491	incubated with secondary anti-rabbit IgG linked with HRP for 1 h, washed and developed using
492	enhanced chemiluminescence substrates. The intensity of immunoblot signals was analyzed
493	and measured with Image J software (Schneider et al., 2012). Statistical analysis was performed
494	using GraphPad Prism software. One-way ANOVA (Dunnett's multiple comparisons test) was
495	used to compare the mean for each variant with the mean for SpA _{ED} wild-type (Figure 1c, 2b).
496	

497 Pulse-labeling

498 Staphylococcal cultures were grown to mid-log phase (OD₆₀₀ 0.8) in TSB and bacteria 499 sedimented by centrifugation at 18,000 $\times q$ for 5 min. Bacterial pellets were washed twice and suspended in 1 ml minimal medium 4. 35 S-methionine/cysteine (100 µl =100 µCi Perkin Elmer) 500 501 was added to bacterial suspensions, vortexed and incubated for 60 seconds at 37°C. 250 µl was 502 removed and immediately mixed with 250 μ l ice-cold 10% TCA to guench all metabolic activity 503 (time 0'). Chase solution (50 μ l of 2 mg/ml methionine, 2 mg/ml cysteine and 10 mg/ml 504 casamino acids) was added to the remainder of bacterial suspension and incubated for 1, 5 and 505 20 min. At each time point, 250 µl bacterial suspension was removed and mixed with 250 µl ice-506 cold 10% TCA. TCA precipitated cells were washed with acetone, dried and suspended in 1 ml 507 0.5 M Tris-HCl (pH 7.0) containing 20 µg/ml lysostaphin. After lysostaphin treatment at 37°C for 508 1 h, cell lysate was precipitated with 7% TCA, washed with acetone, dried, suspended in 50 µl 509 4% SDS, 0.5 M Tris-HCl (pH 7.5) and allowed to incubate for 30 min prior to boiling. 510 Subsequently, samples were incubated for 1 h with rabbit polyclonal anti-SpA_{KKAA} antibody (Kim 511 et al., 2010) that was 1:1000 diluted in 1 ml RIPA buffer (0.1% SDS, 0.5% deoxycholic acid, 1%

512 Triton X-100, 50 mM Tris-HCl pH 8.0, 150 mM NaCl). Protein A sepharose (50 μl of 50% slurry,

513 Sigma) was added to each sample and incubated for 1 h followed by five washes with 1 ml RIPA

514 buffer. Proteins bound to the beads were solubilized by boiling in 15 μ l 2×SDS sample buffer for

515 10 min and separated on 10% (SpA) or 15% SDS-PAGE (SpA_{ED}). Gels were dried on Whatman 3

516 M paper and autoradiographed on X-ray film for 48 hours or longer.

517

518 Purification of SpA_{ED/S18L}, Edman degradation and MALDI-TOF mass spectrometry

519 Overnight bacterial cultures of *S. aureus* WY110 (pSpA_{ED} or its derivatives) were diluted 1: 100 520 into 4 liters of TSB and grown to OD₆₀₀ 2. Staphylococci were sedimented by centrifugation at 521 8,000 $\times q$ for 10 min. Bacteria were suspended in 30 ml of Tris-buffer, 0.5 (vol/vol) 0.1 mm 522 sterilized glass beads were added and peptidoglycan was broken with 15×1 min pulses in a 523 bead-beating instrument (MP Biomedicals). Samples were centrifuged at 7000 $\times q$ for 10 min to 524 sediment glass beads. The supernatant was transferred to another tube and centrifuged at 525 33,000 $\times q$ for 1 hour at 4 °C. The membrane sediment was suspended in 30 ml RIPA buffer and 526 incubated for 1 hour with rotation. RIPA extract was centrifuged at centrifuged at 33,000 $\times q$ for 527 1 hour at 4 °C. The supernatant was removed and subjected to affinity chromatography. Two ml 528 50% suspension of IgG sepharose (GE Healthcare) was loaded onto column. Column bed was 529 washed with 7 ml 0.1 M glycine (pH 3.0), twice with 14 ml 50 mM Tris-HCl (pH 7 .5) and once 530 with 10 ml RIPA buffer. RIPA membrane extracts were loaded onto the column followed with 531 two washes with 14 ml RIPA buffer and once with 10 ml 50 mM Tris-HCl (pH 7 .5). Proteins were 532 eluted by adding four times 1 ml 0.1 M glycine (pH 3.0) to the column and immediately 533 neutralizing the eluate with 25 µl of 1.5 M Tris (pH 8.8). For Edman degradation, the purified

534	SpA _{ED} precursors were 10-fold concentrated via Amicon [®] Ultra-0.5 ml Centrifugal Filters (10 kD
535	cut off). Proteins were separated by 15% SDS-PAGE, electro-transferred to PVDF and stained by
536	Coomassie-Brilliant Blue. Bands of interest were excised and subjected to Edman degradation
537	(Alphalyse, Inc, CA, USA). For MALDI-TOF mass spectrometry analysis, 1 μ l of SpA _{ED} samples
538	were mixed with 1 μl of 10 mg/ml sinapic acid, dried on the Bruker MTP 384 massive plate, and
539	examined in a Bruker Autoflex Speed MALDI-TOF mass spectrometry in the linear positive-ion
540	mode using peptide standards for calibration.

542 Crosslinking of SpA_{ED} precursor

543 Overnight cultures of S. aureus WY110 ($\Delta spa \Delta sbi$, pSpA_{FD/S181}) and S. aureus WY110 ($\Delta spa \Delta sbi$, 544 pSpA_{ED/SP-SasF}) were each diluted 1: 100 into 4 L TSB and grown to OD₆₀₀ 2. Formaldehyde (0.9%, 545 methanol free) was added to the bacterial culture and incubated for 20 min with shaking. 546 Cross-linking was quenched by adding 400 ml ice-cold 0.125 M glycine and rotating the sample 547 for 10 min. Staphylococci were sedimented by centrifugation at 8,000 $\times q$ for 10 min. Bacteria were suspended in 30 ml of 50 mM Tris-HCl (pH 7.5), 150 mM NaCl, and washed twice in the 548 549 same buffer. Sterilized 0.1 mm glass beads 0.5 (vol/vol) were added and peptidoglycan broken 550 with 15×1 min pulses in a bead-beating instrument (MP Biomedicals). Samples were centrifuged at 7000 $\times q$ for 10 min to sediment glass beads. The supernatant was transferred to 551 552 another tube and centrifuged at 33,000 $\times q$ for 1 hour at 4 °C. The membrane sediment was 553 suspended in 30 ml 50 mM Tris-HCl (pH 7 .5), 2% n-dodecyl β-D-maltoside (DDM) and incubated 554 at 4 °C overnight. Samples were subjected to ultracentrifugation at 150,000 $\times q$ for 40 min. The 555 supernatant was subjected to affinity chromatography on IgG sepharose affinity purification as

described above. Eluate was concentrated via Amicon® Ultra-0.5 ml 10 kD Centrifugal Filters
and mixed with equal volume of 2×SDS sample buffer. To reverse the cross-linking, samples
were either boiled at 90°C for 20 min or, as a control, incubated at 60°C (no reversal of crosslinking). Proteins in all samples were separated on 12% SDS-PAGE and bands of interest excised
as indicated in Figure 4 and subjected to protein identification and semi-quantitative analysis at
the Harvard University Taplin Mass Spectrometry Facility (*Table S1*).

562

563 SecA depletion and SecA-sfGFP induction

564 Overnight cultures of S. aureus RN4220 (WT), S. aureus WY223 (Pspac-secA) and S. aureus WY230 565 (Pspac-secA, Ptet-secA:sfGFP) were grown in TSB and 1 mM IPTG. Overnight cultures were washed 566 twice with an equal volume of TSB and diluted 1:100 into fresh TSB with or without 1 mM IPTG 567 and with or without 200 ng/ml ATc. After 3 h growth at 37°C, cultures were diluted into fresh 568 TSB with or without IPTG or ATc and subjected to further growth at 37°C. Growth was 569 monitored by sampling cultures at timed intervals and measuring optical density. One ml 570 bacterial culture was removed after 3 hours (prior to the second 1:100 dilution) and after 6 571 hours (3 hours after the second 1:100 dilution). Samples were processed for protein secretion 572 and immunoblotting assays or analyzed by fluorescence microscopy. A similar procedure was 573 performed for LtaS depletion using S. aureus ANG499 (Pspac-ItaS). Samples from the LtaS 574 depletion experiments were analyzed after 3 hours growth with or without 1 mM IPTG. 575

576 Fluorescence microscopy

577 To observe SpA targeting to the cross-wall, 2 ml mid-log phase S. aureus culture (OD_{600} 0.8) 578 were centrifuged at 18,000 $\times g$ for 5 min, supernatant removed, bacteria washed once in 2 ml 579 PBS and suspended in 1 ml PBS containing 0.5 mg/ml trypsin (Sigma). After incubation at 37°C 580 for 1 hour, staphylococci were washed twice with PBS, suspended in fresh TSB containing 2.5 581 mg/ml soybean trypsin inhibitor (Sigma) and incubated at 37°C for 20 min with rotation. 250 µl 582 of the cell suspension was removed and immediately mixed with fixation solution (2.5% 583 paraformaldehyde and 0.006% glutaraldehyde in PBS). The cells were fixed for 20 min at room 584 temperature, washed three times with PBS and applied to poly-L-lysine coated 8-well glass 585 slides (MP Biomedicals) for 5 min. Excess and non-adherent cells were washed away with PBS. 586 Mobilized cells were blocked with 3% BSA in PBS for 45 min and incubated with SpA-specific 587 mouse hybridoma monoclonal antibody 5A10 (Kim et al., 2010) (diluted 1:4,000 in 3% BSA) for 1 hour. Cells were washed 8 times with PBS and further incubated in dark with Alexa Fluor 647 588 589 conjugated anti-mouse IgG (1:500 in 3% BSA) (Invitrogen) for 1 hour. Cells were washed 10 590 times with PBS and incubated with 1 µg/ml BODIPY-FL vancomycin (ThermoFisher) for 10 min in the dark followed by washing 5 times with PBS. A drop of SlowFade[®] Gold reagent (Molecular 591 592 Probes) was applied to samples before sealing coverslips with nail polish. Fluorescent images 593 were visualized and captured on a Leica SP5 Tandem Scanner Spectral 2-Photon Confocal 594 microscope with 100×oil objective. Identical settings and exposure times were applied to all 595 samples.

To image SpA display on the staphylococcal surface, 1 ml of mid-log phase *S. aureus* cultures were centrifuged at 18,000 $\times g$ for 5 min and supernatant removed. Bacteria were washed once in 2 ml PBS and suspended in 1 ml PBS and mixed with fixation solution. Cells

were fixed for 20 min at room temperature, washed three times with PBS and applied to poly-Llysine coated 8-well glass slides (MP Biomedicals) for 5 min, stained with vancomycin and αSpA
antibodies and analyzed by fluorescence microscopy.

602 To localize intracellular SpA, 2 ml of mid-log phase staphylococcal cultures were 603 centrifuged at 18,000 $\times q$ for 5 min and supernatant removed. Bacteria were washed once in 2 604 ml PBS and suspended in 1 ml PBS, 0.5 mg/ml trypsin (Sigma). After incubation at 37°C for 1 605 hour, staphylococcal cells were washed twice with PBS and fixed with fixation solution. The 606 cells were fixed for 15 min at room temperature and 30 min on ice, washed three times with 607 PBS and suspended in 1 ml GTE buffer [50 mM glucose, 20 mM Tris-HCl (pH 7.5), 10 mM EDTA]. 608 Lysostaphin (10 μ g/ml) was added and 50 μ l cell suspensions were immediately applied to poly-609 L-lysine coated 8-well glass slides and incubated for 1 min. Non-adherent cells were removed 610 and PBS, 0.2% Triton X-100 was applied to samples for 10 seconds. Excessive liquid was 611 aspirated and slides were air-dried. Dried slides were immediately dipped in methanol at -20°C 612 for 5 min, and in acetone at -20°C for 30 s and then allowed to dry completely. Afterwards, the 613 cells on the slides were re-hydrated with PBS for 5 min. blocked with 3% BSA. stained with the 614 membrane dye Nile red (Sigma) and rabbit antibodies specific for SpA followed by Alexa-Fluor-615 488 conjugated goat-anti-rabbit-IgG and analyzed by fluorescence microscopy as described 616 above.

To visualize the sub-cellular localization of SecA-sfGFP, samples from 3 h growth
cultures were removed as described above. Bacteria were sedimented by centrifugation and
washed twice in PBS. Cells were stained with 1 μg/μl FM4-64FX (Molecular Probes) for 10 min
in the dark and were then fixed with fixation solution for 20 min. After washing twice with PBS,

621 cells were applied to poly-L-lysine coated glass slides, SlowFade[®] Gold reagent added,

622 coverslips sealed and samples imaged by fluorescence microscopy.

623	All the images were analyzed in Image J software (Schneider et al., 2012). To quantify
624	the frequency of SpA cross-wall localization at 20 min regeneration after trypsin digestion,
625	numbers of diplococci and numbers of cross-wall localized SpA were counted manually using
626	the cell counter tool in Image J. Diplococci were defined as two daughter cells that had divided
627	and formed a cross-wall but had not yet separated. Cross-wall localized SpA signals were
628	defined as lines at the cross-wall of diplococci. Diplococci were counted in vancomycin stained
629	images and cross-wall localized SpA was counted in merged images. The frequency was
630	determined by dividing cross-wall localized SpA by the number of diplococci. An example of the
631	counting method is displayed in the Source file to Figure 2e. At least two random images were
632	acquired per sample for each experiment. Three or more independent experiments were
633	performed and data from more than 200 diplococci were analyzed for statistically significant
634	differences using one-way ANOVA with Dunnett's multiple comparison test comparing
635	staphylococci expressing wild-type and <i>spa</i> variants (Figure 2e). In <i>Figure 6c</i> and <i>Figure 10c</i> the
636	Tukey's multiple comparison test was used to analyze differences between multiple groups.
637	

638 Acknowledgements

We thank Vytas Bindokas (Microscopy Core Facility, University of Chicago) for assistance with
 microscopy and members of our laboratory for experimental advice and discussion. This work
 was supported by National Institute of Allergy and Infectious Diseases grants Al038897 and

- 642 AI052474. W. Y acknowledges support from German Research Foundation (DFG) Fellowship
- 643 (award YU 181/1-1). The authors declare no conflicts of interest.

645 Figure legends

646	Figure 1.	Mutagenesis of	the signal peptide	of staphylococca	l protein A (S	SpA). (a) Schematic

647 illustrating the primary structure of SpA and of SpA_{ED} with the immunoglobulin binding domains

648 (IgBDs, designated E, A, B, C and D), region X (Xr), LysM domain and LPXTG sorting signal.

649 Cleavage sites for signal peptidase and sortase A are indicated. The amino acid sequence of the

650 SpA signal peptide is displayed. YSIRK/GXXS motif residues are printed in red. (b) The structural

651 genes for SpA_{ED} and its variants were cloned into pOS1, expressed from the *spa* promoter in *S*.

652 *aureus* WY110 (Δ*spa* Δ*sbi*) and secretion of SpA_{ED} was analyzed by immunoblotting with SpA-

653 specific antibody in the culture supernatant (S) and lysostaphin-digested bacterial pellets (P). (c)

654 Percent secretion of wild-type SpA_{ED} and its variants was quantified from triplicate experiments

as the intensity of immunoblotting signals in the supernatant (S) divided by the sum signals in

656 (S+P) fractions ×100. Statistical significance was analyzed with one-way ANOVA comparing each

variant with wild-type and p values were recorded: WT vs. Δ GIAS, p=0.031; WT vs. Δ IA,

658 *p*=0.0032; WT vs. R10A, *p*=0.0116; WT vs. S18L, *p*=0.0172. * denotes *p*<0.05, ** denotes

659 *p*<0.01.

660

Figure 2. SpA signal peptide variants defective in precursor processing and septal secretion. (a)
 S. aureus cultures were fractionated into cytoplasm (C), membrane (M), cell wall (W) and
 culture supernatant (S) and analyzed by immunoblotting with αSpA to reveal the subcellular

664	location of wild-type SpA _{ED} precursor and secreted product of the SpA _{ED/ΔIA, SpA_{ED/S18L}, and}
665	SpA _{ED/R10A} variants. Immunoblotting with $lpha$ SrtA and $lpha$ L6 was used to establish fractionation and
666	loading controls. (b) Quantification of immunoblot signal intensity in (a) using Image J.
667	Precursor abundance (%) the bacterial cytoplasm (C) and membrane (M) was quantified from
668	triplicate experiments as the intensity of immunoblotting signals divided by the sum signals in
669	all four fractions (C+M+W+S) $ imes$ 100. Statistical significance was analyzed with one-way ANOVA
670	comparing each variant with wild-type and <i>p</i> values were recorded: for [C/(C+M+W+S)]×100,
671	WT vs. ΔIA, <i>p</i> <0.0001; WT vs. S18L, <i>p</i> =0.0042; WT vs. R10A, <i>p</i> <0.0001; for [M/(C+M+W+S)]×100,
672	WT vs. ΔIA, <i>p</i> =0.0056; WT vs. S18L, <i>p</i> <0.0001; WT vs. R10A, <i>p</i> =0.0405. **** denotes <i>p</i> <0.0001,
673	** denotes p<0.01, * denotes p<0.05. (c) S. aureus cultures were pulse-labeled for 60 seconds
674	with [³⁵ S]methionine and labeling quenched by adding an excess of non-radioactive methionine
675	(chase). At timed intervals during the pulse (0') or 1 (1'), 5 (5'), and 20 (20') minutes after the
676	pulse (chase), culture aliquots were precipitated with trichloroacetic acid (TCA), lysostaphin-
677	treated, immunoprecipitated with $lpha$ SpA and analyzed by autoradiography. (d) S. aureus WY110
678	(Δ <i>spa</i> Δ <i>sbi</i>) harboring chromosomal pCL55-insertions of wild-type <i>spa</i> (SpA), <i>spa</i> _{ΔIA} (SpA _{ΔIA})
679	spa_{S18L} (SpA _{S18L}), spa_{R10A} (SpA _{R10A}) $spa_{SP-SasF}$ (SpA _{SP-SasF}) or pCL55 alone (Vector) were treated
680	with trypsin to remove SpA. Bacteria were incubated for 20 min to allow for secretion and cell
681	wall deposition of newly synthesized SpA. Samples were incubated with BODIPY-FL vancomycin
682	(Vancomycin) (green) to stain the bacterial cell wall and with SpA-specific monoclonal antibody
683	and Alexa fluor 647-labeled secondary IgG (red) to reveal SpA. (e) SpA-positive staphylococci in
684	images derived from samples in (d) were analyzed for SpA deposition at the cross wall of
685	diplococci (n=200). Data from three independent experiments were used to derive the mean

686	(\pm SEM) and were analyzed for significant differences with one-way ANOVA for comparisons
687	between wild-type and mutant SpA. p values were recorded: SpA vs. SpA _{ΔIA, p<0.0001; SpA vs.}
688	SpA _{S18L} , <i>p</i> =0.0006; SpA vs. SpA _{R10A} , <i>p</i> =0.0004; SpA vs. SpA _{SP-SasF} , <i>p</i> <0.0001; SpA vs. Vector,
689	<i>p</i> <0.0001. **** denotes <i>p</i> <0.0001, *** denotes <i>p</i> <0.001.
690	
691	Figure 3. Proteolytic cleavage of the SpA signal peptide. (a) Wild-type SpA _{ED} or SpA _{ED/ΔIA} ,
692	$SpA_{ED/S18L}$, and $SpA_{ED/R10A}$ variants precursors and cleavage products were purified from
693	detergent-solubilized staphylococcal membranes using affinity chromatography on IgG-
694	sepharose and analyzed on Coomassie-Blue stained SDS-PAGE. Full length precursors (1) and
695	their cleavage products (2-4) were analyzed by Edman degradation and MALDI-TOF mass
696	spectrometry. See Table 1 for mass spectrometry data. (b) Schematic illustrating the proteolytic
697	cleavage sites for each of the four precursors SpA _{ED} , SpA _{ED/ΔIA} , SpA _{ED/S18L} and SpA _{ED/R10A} .
698	
699	Figure 4. Crosslinking of staphylococcal proteins to SpA _{ED/S18L} or SpA _{ED/SP-SasF} . (a) Bacteria from <i>S</i> .
700	aureus WY110 (pSpA _{ED/S18L}) and S. aureus WY110 (pSpA _{ED/SP-SasF}) cultures were crosslinked with
701	0.9% formaldehyde, membrane proteins detergent-solubilized and $SpA_{ED/S18L}$ as well as $SpA_{ED/SP-}$
702	_{SasF} . precursors purified by affinity chromatography on IgG-sepharose. Eluate was treated for 20
703	min at 90°C to reverse cross-linking or kept at 60°C (cross-linked control) and analyzed on
704	Coomassie-stained SDS-PAGE. Bands were excised as indicated and individual proteins
705	identified via ESI-MS analyses of tryptic peptides and data comparison with in silico trypsin-
706	cleaved translation products derived from the genome sequence of S. aureus. Immunoblotting

- of 90°C samples to validate crosslinking of SpA_{ED/S18L} staphylococcal proteins (b) and to SecA (c).
- 708 See Table S1 for a summary of proteins crosslinked to SpA_{ED/S18L}.
- 709
- 710 Figure 5. Depletion of SecA in *S. aureus*. (a) Diagram of the *secA* gene locus in *S. aureus* RN4220
- 711 (wild-type parent, WT) and its P_{spac}-secA variant. (b) Bacteria from overnight cultures of wild-

type S. aureus and S. aureus P_{spac}-secA grown in TSB with 1 mM IPTG were washed and

- suspended in fresh TSB with or without 1 mM IPTG. Subsequent growth was monitored as
- increased absorbance at 600 nm (A₆₀₀). After three hours, cultures were diluted 1:100 into fresh
- 715 TSB with or without 1 mM IPTG and incubated for additional growth measurements. (c) S.

716 *aureus* P_{spac}-secA was streaked on tryptic soy agar with or without 1 mM IPTG supplement and

717 incubated for 16 hours at 37°C for growth. (d) Culture samples retrieved after 3 and 6 hours in

- (b) were analyzed by immunoblotting with antibodies against SecA (α SecA).
- 719

720 Figure 6. SecA depletion diminishes septal secretion of SpA in S. aureus. (a) SpA precursor processing of [³⁵S]methionine pulse-labeled S. aureus RN4220 (WT) or S. aureus P_{spac}-secA 721 722 grown in the presence or absence of 1 mM IPTG. Bacteria were pulse-labeled for 60 sec with 723 radioactive methionine and then incubated with an excess of non-radioactive methionine. 724 During the pulse (0') or 1 (1'), 5 (5') and 20 (20') min after the addition of excess unlabeled 725 methionine, culture aliquots were withdrawn, precipitated with TCA, digested with lysostaphin, 726 and subjected to SDS-PAGE and autoradiography of immunoprecipitated SpA. Wild-type S. 727 aureus (WT) and its P_{spac}-secA variant were grown for 3 (b) and 6 hours (d) in the presence or 728 absence of 1 mM IPTG (see Figure 5) and treated with trypsin to remove SpA from the bacterial

729 surface. Bacteria were incubated for 20 min to allow for secretion and cell wall deposition of 730 newly synthesized SpA. Samples were incubated with BODIPY-FL vancomycin (green) to stain 731 the bacterial cell wall and with SpA-specific monoclonal antibody and Alexa Fluor 647-labeled 732 secondary IgG (red) to reveal SpA. As a control for SpA-specific staining, the S. aureus Δspa 733 variant grown in the absence of IPTG was analyzed by fluorescence microscopy. (c) SpA-positive 734 staphylococci in images derived from samples in (b) were analyzed for SpA deposition at the 735 cross wall of diplococci (n=200). Data from three independent experiments were used to derive 736 the mean (\pm SEM), were analyzed for significant differences with one-way ANOVA and p values 737 were recorded: RN4220-IPTG vs. RN4220+IPTG, non-significant (ns); RN4220-IPTG vs. WY223-738 IPTG, p=0.0003; WY223-IPTG vs. WY223+IPTG, p<0.0001, RN4220+IPTG vs. WY223+IPTG, ns. (e) 739 SecA depletion diminishes secretion of staphylococcal proteins. Protein samples from the 740 extracellular medium and bacterial pellet of S. aureus RN4220 (WT) and S. aureus Psnac-secA 741 cultures grown for 3 hours in the presence or absence of 1 mM IPTG were analyzed by 742 immunoblotting with antibodies against glycerol-ester hydrolase (α Geh), nuclease (α Nuc) and 743 sortase A (α SrtA).

744

Figure 7. SecA localization in staphylococci. (a) Diagram of the *secA* gene locus and of the
pCL55-mediated *att* insertion site for *secA-sfGFP* in the staphylococcal genome. (b) Bacteria
from overnight cultures of *S. aureus* RN4220 (WT), *S. aureus* P_{spac}-secA and *S. aureus* P_{spac}secA/P_{tet}-secA:sfGFP grown in TSB with 1 mM IPTG were washed and suspended in fresh TSB
without IPTG and with or without 1 mM anhydro-tetracycline (ATc); growth was monitored as
increased absorbance at 600 nm (A₆₀₀). After three hours, cultures were diluted 1:100 into fresh

751	TSB without IPTG and with or without 1 mM ATc and incubated for further growth
752	measurements. (c) Culture samples retrieved after 3 and 6 hours from the experiment detailed
753	in (b) were analyzed by immunoblotting with rabbit antibodies against SecA ($lpha$ SecA) and sfGFP
754	($lpha$ GFP). (d) [³⁵ S]methionine-labeled <i>S. aureus</i> cultures incubated for three hours as described in
755	(b) were analyzed during the 60 sec pulse with radioactive methionine (0) and 1, 5 and 20 min
756	after the addition of excess unlabeled methionine via SDS-PAGE and autoradiography of
757	immunoprecipitated SpA. (e) Fluorescence microscopy of bacteria from S. aureus cultures
758	incubated for three hours as described in (b). Bacteria were stained with the membrane dye
759	FM4-64 (red) and analyzed for SecA-sfGFP fluorescence (green).
760	
761	Figure 8. Intracellular trafficking of SpA in the presence and absence of SecA. (a) S. aureus P _{spac} -
762	secA cells were grown in the presence (+SecA) or absence of 1 mM IPTG (-SecA) and, alongside
763	S. aureus Δspa control cells, were trypsin treated to remove extracellular surface proteins and
764	fixed with para-formaldehyde. Samples were then treated with lysostaphin (+Lysostaphin) or
765	left untreated (-Lysostaphin), incubated with detergent and SpA-specific rabbit antibodies and
766	Alexa Fluor 488-labeled goat-anti-rabbit-IgG (green) and with Nile red to reveal bacterial
767	membranes. Bright-field microscopy (BF) images were acquired to reveal the contours of all
768	bacterial cells. Scale bar, 1 μ m. (b) Additional samples (#1, #2 and #3) of <i>S. aureus</i> P _{spac} -secA
769	cells were grown in the presence of 1 mM IPTG (+SecA), trypsin treated, fixed with
770	formaldehyde, lysostaphin treated, incubated with detergent and with SpA-specific antibody
771	(green) and Nile red.

773 Figure 9. SecDF is required for SpA trafficking to septal membranes. (a) S. qureus cultures were 774 centrifuged to sediment the bacteria into a pellet (P) and separate them from the extracellular 775 medium (S, supernatant). Following lysostaphin digestion of bacteria, proteins in both fractions 776 were precipitated with TCA and analyzed by immunoblotting with α SpA. (b) S. aureus cultures 777 were fractionated as described in (a) and subjected to immunoblotting with antibodies specific 778 for glycerol-ester hydrolase (α Geh), coagulase (α Coa) and sortase A (α SrtA). (c) Fluorescence 779 microscopy of bacteria from cultures of S. aureus RN4220 (WT, wild-type), WY418 (Δ secDF), 780 WY416 ($\Delta rnd2$), WY400 ($\Delta rnd3$) and WY412 ($\Delta secDF \Delta rnd23$) mutants with and without 781 expression plasmid for wild-type secDF (pSecDF) as well as S. aureus SEJ1 (Δ spa) as control. 782 Bacteria were trypsin treated to remove extracellular surface proteins and fixed with para-783 formaldehyde. Samples were treated with lysostaphin, incubated with detergent and SpA-784 specific rabbit antibodies and Alexa Fluor 488-labeled goat-anti-rabbit-IgG (green) and with Nile 785 red to reveal bacterial membranes. BF identifies the bright-field microscopy view of 786 fluorescence microscopy images. Scale bar, 1 µm. 787 788 Figure 10. Localization of SpA secretion in LtaS-depleted S. aureus. (a) Schematic to illustrate 789 the ItaS locus in S. aureus RN4220 and ANG499. (b) Fluorescence microscopy with BODIPY-FL-790 vancomycin (green) and α SpA (red) stained samples 20 min after trypsin removal of surface 791 proteins from the staphylococcal envelope to detect newly synthesized SpA. Scale bar, 2 μ m. (c) 792 SpA-positive staphylococci in images derived from samples in (b) were analyzed for SpA

793 deposition at the cross wall of diplococci (n=200). Data from three independent experiments

vere used to derive the mean (±SEM) and were analyzed for significant differences with one-

795	way ANOVA for comparisons between <i>S. aureus</i> RN4220 (WT) and ANG499 grown with (+LtaS)
796	and without IPTG (-LtaS). <i>p</i> values were recorded: RN4220-IPTG vs. ANG499-IPTG, <i>p</i> <0.0001;
797	ANG499-IPTG vs. ANG499+IPTG, p < 0.0001. (d) Fluorescence microscopy to localize intracellular
798	SpA in <i>S. aureus</i> strains RN4220 (WT) and ANG499 (P _{spac} -ItaS) grown with and without IPTG
799	induction for 3 hours. Bacteria were trypsin treated to remove extracellular surface proteins
800	and fixed with para-formaldehyde. Samples were then treated with lysostaphin, incubated with
801	detergent and SpA-specific rabbit antibodies and Alexa Fluor 488-labeled goat-anti-rabbit-IgG
802	(green) and with Nile red to reveal bacterial membranes. BF identifies the bright-field
803	microscopy view of fluorescence microscopy images. Scale bar, 2 μ m. (e) The culture
804	supernatant (S) and bacterial pellet (P) samples of <i>S. aureus</i> RN4220 and ANG499 grown for
805	three hours in the presence or absence of IPTG were immunoblotted with antibodies specific
806	for SpA ($lpha$ SpA), glycerol-ester hydrolase ($lpha$ Geh), coagulase ($lpha$ Coa), nuclease ($lpha$ Nuc) and sortase
807	A ($lpha$ SrtA). (f) Fluorescence microscopy of staphylococci to measure surface display of protein A
808	in bacteria stained with BODIPY-FL-vancomycin (Van-FL) (green) and $lpha$ SpA (red) without trypsin
809	treatment. Scale bar, 2 μm.

810

811 References

812	ABRAHMSÉN, L., MOKS, T., NILSSON, B., HELLMAN, U. & UHLÉN, M. 1985. Analysis of signals for
813	secretion in the staphylococcal protein A gene. EMBO J., 4, 3901-3906.

- BAE, T., BANGER, A. K., WALLACE, A., GLASS, E. M., ASLUND, F., SCHNEEWIND, O. & MISSIAKAS,
 D. M. 2004. Staphylococcus aureus virulence genes identified by bursa aurealis
 mutagenesis and nematode killing. *Proc Natl Acad Sci U S A*, 101, 12312-7.
- BAE, T. & SCHNEEWIND, O. 2003. The YSIRK-G/S motif of staphylococcal protein A and its role in
 efficiency of signal peptide processing. *J. Bacteriol.*, 185, 2910-2919.
- BAE, T. & SCHNEEWIND, O. 2006. Allelic replacement in Staphylococcus aureus with inducible
 counter-selection. *Plasmid*, 55, 58-63.

821 BREGA, S., CALIOT, E., TRIEU-CUOT, P. & DRAMSI, S. 2013. SecA localization and SecA-822 dependent secretion occurs at new division septa in group B streptococcus. PLoS One, 8, 823 e65832. 824 CAMPO, N., TJALSMA, H., BUIST, G., STEPNIAK, D., MEIJER, M., VEENHUIS, M., WESTERMANN, 825 M., MULLER, J. P., BRON, S., KOK, J., KUIPERS, O. P. & JONGBLOED, J. D. 2004. 826 Subcellular sites for bacterial protein export. Mol. Microbiol., 53, 1583-1599. 827 CARLSSON, F., STALHAMMAR-CARLEMALM, M., FLARDH, K., SANDIN, C., CARLEMALM, E. & 828 LINDAHL, G. 2006. Signal sequence directs localized secretion of bacterial surface 829 proteins. Nature, 442, 943-946. 830 CHENG, A. G., MISSIAKAS, D. M. & SCHNEEWIND, O. 2014. The giant protein Ebh is a cross wall 831 determinant of Staphylococcus aureus cell size and complement resistance. J. Bacteriol., 832 196, 971-981. 833 COLE, R. M. & HAHN, J. J. 1962. Cell wall replication in Streptococcus pyogenes. Science, 135, 834 722-724. 835 DEDENT, A. C., MCADOW, M. & SCHNEEWIND, O. 2007. Distribution of protein A on the surface 836 of Staphylococcus aureus. J. Bacteriol., 189, 4473-4484. 837 DEDENT, A. C., MISSIAKAS, D. M. & SCHNEEWIND, O. 2008. Signal peptides direct surface 838 proteins to two distinct envelope locations of Staphylococcus aureus. EMBO J., 27, 2656-2668. 839 840 EMR, S. D., HANLEY-WAY, S. & SILHAVY, T. J. 1981. Suppressor mutations that restore export of 841 a protein with a defective signal sequence. *Cell*, 23, 79-88. 842 EMR, S. D., SCHWARTZ, M. & SILHAVY, T. J. 1978. Mutations altering the cellular localization of 843 the phage lambda receptor, an Escherichia coli outer membrane protein. Proc. Natl. 844 Acad. Sci USA, 75, 5802-6. 845 FORSGREN, A. & SJÖQUIST, J. 1966. Protein A from S. aureus. I. Pseudo-immune reaction with 846 human gamma-globulin. J. Immunol., 97, 822-827. 847 FOSTER, T. J., GEOGHEGAN, J. A., GANESH, V. K. & HÖÖK, M. 2014. Adhesion, invasion and 848 evasion: the many functions of the surface proteins of Staphylococcus aureus. Nat. Rev. 849 Microbiol., 12, 49-62. 850 FRANKEL, M. B., HENDRICKX, A. P., MISSIAKAS, D. M. & SCHNEEWIND, O. 2011. LytN, a murein 851 hydrolase in the cross-wall compartment of Staphylococcus aureus, is involved in proper 852 bacterial growth and envelope assembly. J. Biol. Chem., 286, 32593-32605. 853 GARDEL, C., BENSON, S., HUNT, J., MICHAELIS, S. & BECKWITH, J. 1987. secD, a new gene 854 involved in protein export in Escherichia coli. J. Bacteriol., 169, 1286-1290. 855 GIESBRECHT, P., WECKE, J. & REINICKE, B. 1976. On the morphogenesis of the cell wall of 856 staphylococci. Int. Rev. Cytol., 44, 225-318. 857 GRÜNDLING, A. & SCHNEEWIND, O. 2007. Synthesis of glycerol phosphate lipoteichoic acid in 858 Staphylococcus aureus. Proc. Nat. Acad. Sci. USA, 104, 8478-8483. 859 HANAHAN, D. 1983. Studies on transformation of Escherichia coli with plasmids. J Mol Biol, 166, 860 557-80. 861 HARRY, E. J., POGLIANO, K. & LOSICK, R. 1995. Use of immunofluorescence to visualize cell-862 specific gene expression during sporulation in Bacillus subtilis. J. Bacteriol., 177, 3386-863 3393.

HU, P., BIAN, Z., FAN, M., HUANG, M. & ZHANG, P. 2008. Sec translocase and sortase A are
colocalised in a locus in the cytoplasmic membrane of *Streptococcus mutans*. *Arch. Oral Biol.*, 53, 150-154.

- KIM, H. K., CHENG, A. G., KIM, H. Y., MISSIAKAS, D. M. & SCHNEEWIND, O. 2010. Nontoxigenic
 protein A vaccine for methicillin-resistant Staphylococcus aureus infections in mice. J
 Exp Med, 207, 1863-70.
- KIM, H. K., FALUGI, F., MISSIAKAS, D. & SCHNEEWIND, O. 2016. Peptidoglycan-linked protein A
 promotes T-cell dependent antibody expansion during *Staphylococcus aureus* infection.
 Proc. Natl. Acad. Sci. USA, 113, 5718-5723.
- KLINE, K. A., KAU, A. L., CHEN, S. L., LIM, A., PINKNER, J. S., ROSCH, J., NALLAPAREDDY, S. R.,
 MURRAY, B. E., HENRIQUES-NORMARK, B., BEATTY, W., CAPARON, M. G. & HULTGREN,
 S. J. 2009. Mechanism for sortase localization and the role of sortase localization in
 efficient pilus assembly in *Enterococcus faecalis*. J. Bacteriol., 191, 3237-3247.
- KREISWIRTH, B. N., LOFDAHL, S., BETLEY, M. J., O'REILLY, M., SCHLIEVERT, P. M., BERGDOLL, M.
 S. & NOVICK, R. P. 1983. The toxic shock syndrome exotoxin structural gene is not
 detectably transmitted by a prophage. *Nature*, 305, 709-12.
- LEE, C. Y., BURANEN, S. L. & YE, Z. H. 1991. Construction of single-copy integration vectors for
 Staphylococcus aureus. Gene, 103, 101-5.
- LEE, C. Y. & IANDOLO, J. J. 1986. Lysogenic conversion of staphylococcal lipase is caused by
 insertion of the bacteriophage L54a genome into the lipase structural gene. *J. Bacteriol.*,
 166, 385-391.
- LUTKENHAUS, J. 1993. FtsZ ring in bacterial cytokinesis. *Mol. Microbiol.*, 9, 403-409.
- MANN, P. A., MÜLLER, A., XIAO, L., PEREIRA, P. M., YANG, C., HO LEE, S., WANG, H., TRZECIAK,
 J., SCHNEEWEIS, J., DOS SANTOS, M. M., MURGOLO, N., SHE, X., GILL, C., BALIBAR, C. J.,
 LABROLI, M., SU, J., FLATTERY, A., SHERBORNE, B., MAIER, R., TAN, C. M., BLACK, T.,
 ONDER, K., KARGMAN, S., MONSMA, F. J. J., PINHO, M. G., SCHNEIDER, T. & ROEMER, T.
- 890 2013. Murgocil is a highly bioactive staphylococcal-specific inhibitor of the
- peptidoglycan glycosyltransferase enzyme MurG. ACS Chem. Biol., EPub, ahead of print.
 MAZMANIAN, S. K., LIU, G., TON-THAT, H. & SCHNEEWIND, O. 1999. Staphylococcus aureus
- sortase, an enzyme that anchors surface proteins to the cell wall. *Science*, 285, 760-763.
- MONK, I. R., SHAH, I. M., XU, M., TAN, M. W. & FOSTER, T. J. 2012. Transforming the
 untransformable: application of direct transformation to manipulate genetically
 Staphylococcus aureus and Staphylococcus epidermidis. *MBio*, 3.
- MONTEIRO, J. M., FERNANDES, P. B., VAZ, F., PEREIRA, A. R., TAVARES, A. C., FERREIRA, M. T.,
 PEREIRA, P. M., VEIGA, H., KURU, E., VANNIEUWENHZE, M. S., BRUN, Y. V., FILIPE, S. R. &
 PINHO, M. G. 2015. Cell shape dynamics during the staphylococcal cell cycle. *Nat. Commun.*, 6, 8055.
- NAVARRE, W. W. & SCHNEEWIND, O. 1994. Proteolytic cleavage and cell wall anchoring at the
 LPXTG motif of surface proteins in gram-positive bacteria. *Mol. Microbiol.*, 14, 115-121.
- 903 OLIVER, D. B. & BECKWITH, J. 1981. *E. coli* mutant pleiotropically defective in the export of secreted
 904 proteins. *Cell*, 25, 765-772.

905 PEDELACQ, J. D., CABANTOUS, S., TRAN, T., TERWILLIGER, T. C. & WALDO, G. S. 2006. 906 Engineering and characterization of a superfolder green fluorescent protein. *Nat.*907 *Biotechnol.*, 24, 79-88.

- PERCY, M. G. & GRÜNDLING, A. 2014. Lipoteichoic acid synthesis and function in gram-positive
 bacteria. Annu. Rev. Microbiol., 68, 81-100.
- PERRY, A. M., TON-THAT, H., MAZMANIAN, S. K. & SCHNEEWIND, O. 2002. Anchoring of surface
 proteins to the cell wall of *Staphylococcus aureus*. III. Lipid II is an *in vivo* peptidoglycan
 substrate for sortase-catalyzed surface protein anchoring. *J. Biol. Chem.*, 277, 16241 16248.
- 914 PHONIMDAENG, P., O'REILLY, M., NOWLAN, P., BRAMLEY, A. J. & FOSTER, T. J. 1990. The
 915 coagulase of *Staphylococcus aureus* 8325-4. Sequence analysis and virulence of site916 specific coagulase-deficient mutants. *Mol. Microbiol.*, 4, 393-404.
- PINHO, M. G. & ERRINGTON, J. 2003. Dispersed mode of *Staphylococcus aureus* cell wall
 synthesis in the absence of the division machinery. *Mol. Microbiol.*, 50, 871-881.
- PINHO, M. G. & ERRINGTON, J. 2005. Recruitment of penicillin-binding protein PBP2 to the
 division site of *Staphylococcus aureus* is dependent on its transpeptidation substrates.
 Mol. Microbiol., 55, 799-807.
- POGLIANO, J. A. & BECKWITH, J. 1994. SecD and SecF facilitate protein export in *Escherichia coli. EMBO J.,* 13, 554-561.
- QUIBLIER, C., SEIDL, K., ROSCHITZKI, B., ZINKERNAGEL, A. S., BERGER-BÄCHI, B. & SENN, M. M.
 2013. Secretome analysis defines the major role of SecDF in *Staphylococcus aureus*virulence. *PLoS One*, 8, e63513.
- 927 QUIBLIER, C., ZINKERNAGEL, A. S., SCHUEPBACH, R. A., BERGER-BÄCHI, B. & SENN, M. M. 2011.
 928 Contribution of SecDF to *Staphylococcus aureus* resistance and expression of virulence
 929 factors. *BMC Microbiol.*, 11, 72.
- RAVIPATY, S. & REILLY, J. P. 2010. Comprehensive characterization of methicillin-resistant
 Staphylococcus aureus subsp. *aureus* COL secretome by two-dimensional liquid
 chromatography and mass spectrometry. *Mol. Cell. Proteomics*, 9, 1898-1919.
- REICHMANN, N. T., PIÇARRA CASSONA, C., MONTEIRO, J. M., BOTTOMLEY, A. L., CORRIGAN, R.
 M., FOSTER, S. J., PINHO, M. G. & GRÜNDLING, A. 2014. Differential localization of LTA
 synthesis proteins and their interaction with the cell division machinery in *Staphylococcus aureus. Mol. Microbiol.*, 92, 273-286.
- ROHRER, S., EHLERT, K., TSCHIERSKE, M., LABISCHINSKI, H. & BERGER-BÄCHI, B. 1999. The
 essential *Staphylococcus aureus* gene *fmhB* is involved in the first step of peptidoglycan
 pentaglycine interpeptide formation. *Proc. Natl. Acad. Sci. USA*, 96, 9351-9356.
- ROSCH, J. & CAPARON, M. 2004. A microdomain for protein secretion in Gram-positive bacteria.
 Science, 304, 1513-1515.
- ROSENSTEIN, R. & GÖTZ, F. 2000. Staphylococcal lipases:biochemical and molecular
 characterization. *Biochimie*, 82, 1005-1014.
- SCHALLENBERGER, M. A., NIESSEN, S., SHAO, C., FOWLER, B. J. & ROMESBERG, F. E. 2012. Type I
 signal peptidase and protein secretion in *Staphylococcus aureus*. *J. Bacteriol.*, 194, 26772686.
- SCHNEEWIND, O., FOWLER, A. & FAULL, K. F. 1995. Structure of the cell wall anchor of surface
 proteins in *Staphylococcus aureus*. *Science*, 268, 103-106.
- SCHNEEWIND, O., MIHAYLOVA-PETKOV, D. & MODEL, P. 1993. Cell wall sorting signals in
 surface proteins of gram-positive bacteria. *EMBO J*, 12, 4803-11.

- SCHNEEWIND, O. & MISSIAKAS, D. 2014. Genetic manipulation of Staphylococcus aureus. *Curr Protoc Microbiol*, 32, Unit 9C 3.
- SCHNEEWIND, O., MODEL, P. & FISCHETTI, V. A. 1992. Sorting of protein A to the staphylococcal
 cell wall. *Cell*, 70, 267-281.
- SCHNEIDER, C. A., RASBAND, W. S. & ELICEIRI, K. W. 2012. NIH Image to ImageJ: 25 years of
 image analysis. *Nat Methods*, 9, 671-5.
- 957 SHORTLE, D. 1983. A genetic system for analysis of staphylococcal nuclease. *Gene*, 22, 181-189.
- STEELE, V. R., BOTTOMLEY, A. L., GARCIA-LARA, J., KASTURIARACHCHI, J. & FOSTER, S. J. 2011.
 Multiple essential roles for EzrA in cell division of *Staphylococcus aureus*. *Mol. Microbiol.*, 80, 542-555.
- 961 TETTELIN, H., MASIGNANI, V., CIESLEWICZ, M. J., DONATI, C., MEDINI, D., WARD, N. L.,
- 962 ANGIUOLI, S. V., CRABTREE, J., JONES, A. L., DURKIN, A. S., DEBOY, R. T., DAVIDSEN, T.
- 963 M., MORA, M., SCARSELLI, M., MARGARIT Y ROS, I., PETERSON, J. D., HAUSER, C. R.,
- 964 SUNDARAM, J. P., NELSON, W. C., MADUPU, R., BRINKAC, L. M., DODSON, R. J.,
- 965 ROSOVITZ, M. J., SULLIVAN, S. A., DAUGHERTY, S. C., HAFT, D. H., SELENGUT, J., GWINN,
 966 M. L., ZHOU, L., ZAFAR, N., KHOURI, H., RADUNE, D., DIMITROV, G., WATKINS, K.,
- 967 O'CONNOR, K. J., SMITH, S., UTTERBACK, T. R., WHITE, O., RUBENS, C. E., GRANDI, G.,
- 968 MADOFF, L. C., KASPER, D. L., TELFORD, J. L., WESSELS, M. R., RAPPUOLI, R. & FRASER, C.
- M. 2005. Genome analysis of multiple pathogenic isolates of *Streptococcus agalactiae*:
 implications for the microbial "pan-genome". *Proc. Natl. Acad. Sci. USA*, 102, 1395013955.
- TON-THAT, H., FAULL, K. F. & SCHNEEWIND, O. 1997. Anchor structure of staphylococcal
 surface proteins. I. A branched peptide that links the carboxyl terminus of proteins to
 the cell wall. J. Biol. Chem., 272, 22285-22292.
- TON-THAT, H., LIU, G., MAZMANIAN, S. K., FAULL, K. F. & SCHNEEWIND, O. 1999. Purification
 and characterization of sortase, the transpeptidase that cleaves surface proteins of
 Staphylococcus aureus at the LPXTG motif. *Proc. Natl. Acad. Sci. USA*, 96, 12424-12429.
- TON-THAT, H., MAZMANIAN, H., FAULL, K. F. & SCHNEEWIND, O. 2000. Anchoring of surface
 proteins to the cell wall of *Staphylococcus aureus*. I. Sortase catalyzed *in vitro*transpeptidation reaction using LPXTG peptide and NH₂-Gly₃ substrates. *J. Biol. Chem.*,
 275, 9876-9881.
- TON-THAT, H. & SCHNEEWIND, O. 1999. Anchor structure of staphylococcal surface proteins.
 IV. Inhibitors of the cell wall sorting reaction. *J. Biol. Chem.*, 274, 24316-24320.
- 984TOUHAMI, A., JERICHO, M. H. & BEVERIDGE, T. J. 2004. Atomic force microscopy of cell growth985and division in Staphylococcus aureus. J. Bacteriol., 186, 3286-3295.
- TSIRIGOTAKI, A., DE GEYTER, J., ŠOŠTARIC, N., ECONOMOU, A. & KARAMANOU, S. 2017. Protein
 export through the bacterial Sec pathway. *Nat. Rev. Microbiol.*, 15, 21-36.
- TSUI, H. C., KEEN, S. K., SHAM, L. T., WAYNE, K. J. & WINKLER, M. E. 2011. Dynamic distribution
 of the SecA and SecY translocase subunits and septal localization of the HtrA surface
 chaperone/protease during *Streptococcus pneumoniae* D39 cell division. *MBio*, 2,
 e00202-11.
- TSUKAZAKI, T., MORI, H., ECHIZEN, Y., ISHITANI, R., FUKAI, S., TANAKA, T., PEREDERINA, A.,
 VASSYLYEV, D. G., KOHNO, T., MATURANA, A. D., ITO, K. & NUREKI, O. 2011. Structure

- and function of a membrane component SecDF that enhances protein export. *Nature*,474, 235-238.
- TZAGOLOFF, H. & NOVICK, R. 1977. Geometry of cell division in *Staphylococcus aureus*. *J. Bacteriol.*, 129, 343-350.
- 998 UHLÉN, M., GUSS, B., NILSSON, B., GOTZ, F. & LINDBERG, M. 1984. Expression of the gene
 999 encoding protein A in *Staphylococcus aureus* and coagulase-negative staphylococci. *J.* 1000 *Bacteriol*, 159, 713-719.
- VON HEIJNE, G. 1986. Towards a comparative anatomy of N-terminal topogenic protein
 sequences. J. Mol. Biol., 189, 239-42.
- 1003 YU, W. & GÖTZ, F. 2012. Cell wall antibiotics provoke accumulation of anchored mCherry in the 1004 cross wall of *Staphylococcus aureus*. *PLoS One*, **7**, e30076.

1005

1007

Table 1. MALDI-TOF-MS ion signals of purified SpA_{ED} species and their variants Observed m/z^aCalculated *m/z* Protein $\Delta obs.-calc.$ 16776.47 16777.7 1.23 $SpA_{ED}-1$ SpA_{ED}-2 15273.92 15273.78 0.14 SpA_{ED}-3 14418.92 14418.78 0.14 13152.40 13152.32 0.08 SpA_{ED}-4 16803.78 0.76 SpA_{ED/S18L}-1 16803.02 15298.89 15299.86 0.97 SpA_{ED/S18L}-2 14417.89 14418.78 0.89 SpA_{ED/S18L}-3 13152.22 13152.32 0.10 SpA_{ED/S18L}-4 16593.46 0.51 $SpA_{ED/\Delta IA}$ -1 16592.95 $SpA_{ED/\Delta IA}$ -2 15088.71 15089.54 0.83 $SpA_{ED/\Delta IA}$ -3 14417.86 14418.78 0.92 13151.55 13152.32 0.77 $SpA_{ED/\Delta IA}-4$ 0.40 SpA_{ED/R10A}-1 16692.99 16692.59 15584.97 15586.2 1.23 SpA_{ED/R10A}-2 0.32 SpA_{ED/R10A}-3 14418.46 14418.78 SpA_{ED/R10A}-4 13152.07 13152.32 0.25

^aBased on average mass calculated with the online ExPASy tool.

1008

1010 1011

Table S1. List of ESI-MS identified tryptic peptides crosslinked to $SpA_{ED/S18L}$

Number	Gene Locus or Symbol	UniProt reference
of		
peptides		
26	secA	(O06446_SECA_STAA8)
21	alaS	(Q2FXV9_SYA_STAA8)
18	murG	(Q2FYL5_MURG_STAA8)
15	polA	(Q2FXN9_Q2FXN9_STAA8)
15	SAOUHSC_01854	(Q2G245_Q2G245_STAA8)
15	femA	(Q2FYR2_FEMA_STAA8)
11	clpC	(Q2G0P5_CLPC_STAA8)
10	SAOUHSC_01810	(Q2FXM5_Q2FXM5_STAA8)
10	ezrA	(Q2FXK8_EZRA_STAA8)
9	pbp2	(Q2FYI0_Q2FYI0_STAA8)
9	murE2	(Q2FWZ9_Q2FWZ9_STAA8)
9	UDP-N-acetylglucosamine	(Q2FW81_URTF_STAA8)
	pyrophosphorylase	
9	femB	(Q2FYR1_FEMB_STAA8)
9	tagB	(Q2G1C2_Q2G1C2_STAA8)
8	tagF	(Q2G1C1_Q2G1C1_STAA8)
7	ItaS	(Q2G093_LTAS_STAA8)
7	femX	(Q2FVZ4_FEMX_STAA8)
6	1-acyl-sn-glycerol-3-phosphate	(Q2FXJ7_Q2FXJ7_STAA8)
	acyltransferases domain	
	protein	
6	purL	(Q2FZJ0_PURL_STAA8)
6	Conserved hypothetical phage	(Q2FY82_Q2FY82_STAA8)

protein

6	SAOUHSC_02447	(Q2G2D7_Q2G2D7_STAA8)
6	SAOUHSC_01347	(Q2FYS9_Q2FYS9_STAA8)
6	SAOUHSC_01180	(Q2G264_Q2G264_STAA8)
5	clpB	(Q2FZS8_Q2FZS8_STAA8)
5	dltD	(Q2FZW3_Q2FZW3_STAA8)
5	cshA	(Q2FWH5_Y2316_STAA8)
5	prfC	(Q2FZP4_RF3_STAA8)
5	parE	(Q2FYS5_PARE_STAA8)
5	parC	(Q2FYS4_PARC_STAA8)
5	betA	(Q2FV11_BETA_STAA8)
5	SAOUHSC_02417	(Q2FW86_Q2FW86_STAA8)
5	SAOUHSC_02274	(Q2FWL5_Q2FWL5_STAA8)
5	SAOUHSC_01960	(Q2FXA5_Q2FXA5_STAA8)
5	SAOUHSC_01908	(Q2G1W5_Q2G1W5_STAA8)
5	SAOUHSC_01613	(Q2FY52_Q2FY52_STAA8)
5	SAOUHSC_01026	(Q2FZH8_Q2FZH8_STAA8)
5	SAOUHSC_00309	(Q2G146_Q2G146_STAA8)
5	SAOUHSC_00113	(Q2G1K9_Q2G1K9_STAA8)
4	saeS	(Q2G2U1_SAES_STAA8)
4	rplK	(POAOF4_RL11_STAA8)
4	rpIE	(Q2FW18_RL5_STAA8)
4	murC	(Q2FXJ0_MURC_STAA8)
4	metN2	(Q2FZZ2_METN2_STAA8)
4	lip2	(Q2G155_LIP2_STAA8)
4	SAOUHSC_02859	(Q2FV77_Q2FV77_STAA8)
4	SAOUHSC_02582	(Q2FVV9_FDHL_STAA8)
4	SAOUHSC_02363	(Q2FWD6_ALD1_STAA8)
4	SAOUHSC_01884	(Q2FXG3_Q2FXG3_STAA8)

4	SAOUHSC_01855	(Q2G247_Y1855_STAA8)
4	SAOUHSC_01723	(Q2FXV8_Q2FXV8_STAA8)
4	SAOUHSC_01679	(Q2FXZ6_Q2FXZ6_STAA8)
4	SAOUHSC_01460	(Q2FYI6_Q2FYI6_STAA8)
4	SAOUHSC_01321	(Q2FYV3_Q2FYV3_STAA8)
4	SAOUHSC_00893	(Q2FZU7_Q2FZU7_STAA8)
4	SAOUHSC_00637	(Q2G2L2_Q2G2L2_STAA8)
4	SAOUHSC_00531	(Q2G0M9_Q2G0M9_STAA8)
3	tgt	(Q2FXT6_TGT_STAA8)
3	queA	(Q2FXT5_QUEA_STAA8)
3	prs	(Q2G0S2_Q2G0S2_STAA8)
3	pcrA	(Q53727_PCRA_STAA8)
3	hemE	(Q2FXA3_DCUP_STAA8)
3	gyrA	(Q2G2Q0_GYRA_STAA8)
3	gpsA	(Q2FYG1_GPDA_STAA8)
3	glmU	(Q2G0S3_GLMU_STAA8)
3	SAOUHSC_02684	(Q2FVL8_Q2FVL8_STAA8)
3	SAOUHSC_02627	(Q2G2W3_Q2G2W3_STAA8)
3	SAOUHSC_02317	(Q2FWH4_Q2FWH4_STAA8)
3	SAOUHSC_02134	(Q2G234_Q2G234_STAA8)
3	SAOUHSC_01973	(Q2G2T1_Q2G2T1_STAA8)
3	SAOUHSC_01728	(Q2FXV3_Q2FXV3_STAA8)
3	SAOUHSC_01673	(Q2FY01_Q2FY01_STAA8)
3	SAOUHSC_01612	(Q2FY53_Q2FY53_STAA8)
3	SAOUHSC_01584	(Q2FY81_Q2FY81_STAA8)
3	SAOUHSC_01499	(Q2FYF3_Q2FYF3_STAA8)
3	SAOUHSC_01490	(Q2FYG2_Q2FYG2_STAA8)
3	SAOUHSC_01071	(Q2FZF9_Q2FZF9_STAA8)
3	SAOUHSC_00875	(Q2FZW0_Q2FZW0_STAA8)

3	SAOUHSC_00756	(Q2G065_Q2G065_STAA8)
3	SAOUHSC_00731	(Q2G089_Q2G089_STAA8)
3	SAOUHSC_00584	(Q2G0I1_Q2G0I1_STAA8)
3	SAOUHSC_00480	(Q2G0R6_Q2G0R6_STAA8)
3	SAOUHSC_00467	(Q2G0S7_Q2G0S7_STAA8)
3	SAOUHSC_00139	(Q2G1I3_Q2G1I3_STAA8)
2	pknB	(Q2FZ64_Q2FZ64_STAA8)
2	tsaD	(Q2FWL2_TSAD_STAA8)
2	topB	(Q2FW03_TOP3_STAA8)
2	topA	(Q2FZ32_TOP1_STAA8)
2	rsmH	(P60393_RSMH_STAA8)
2	rsmA	(Q2G0T0_RSMA_STAA8)
2	rpsG	(P48940_RS7_STAA8)
2	rpsC	(Q2FW12_RS3_STAA8)
2	rplM	(Q2FW38_RL13_STAA8)
2	rpli	(Q2G2T3_RL9_STAA8)
2	rplF	(Q2FW21_RL6_STAA8)
2	potA	(Q2G2A7_POTA_STAA8)
2	mutS	(Q2FYZ9_MUTS_STAA8)
2	murE	(Q2FZP6_MURE_STAA8)
2	lysA	(Q2FYN4_Q2FYN4_STAA8)
2	gcvT	(Q2FY33_GCST_STAA8)
2	fmt	(Q2FZ68_FMT_STAA8)
2	ebpS	(Q2FYF1_EBPS_STAA8)
2	dnaJ	(Q2FXZ3_DNAJ_STAA8)
2	atpG	(Q2FWE9_Q2FWE9_STAA8)
2	aroC	(Q2FYG9_AROC_STAA8)
2	alr1	(Q9ZAH5_ALR1_STAA8)
2	ald2	(Q2FXL7_DHA2_STAA8)

2	SAOUHSC_02980	(Q2G220_Q2G220_STAA8)
2	SAOUHSC_02899	(Q2FV40_Q2FV40_STAA8)
2	SAOUHSC_02875	(Q2FV62_Q2FV62_STAA8)
2	SAOUHSC_02382	(Q2FWB6_Q2FWB6_STAA8)
2	SAOUHSC_02145	(Q2FWX6_Q2FWX6_STAA8)
2	SAOUHSC_02133	(Q2G235_Q2G235_STAA8)
2	SAOUHSC_01998	(Q2G281_Q2G281_STAA8)
2	SAOUHSC_01816	(Q2FXL9_Y1816_STAA8)
2	SAOUHSC_01794	(Q2FXP2_Q2FXP2_STAA8)
2	SAOUHSC_01791	(Q2FXP5_Q2FXP5_STAA8)
2	SAOUHSC_01766	(Q2FXR9_Q2FXR9_STAA8)
2	SAOUHSC_01660	(Q2FY14_Q2FY14_STAA8)
2	SAOUHSC_01615	(Q2FY50_Q2FY50_STAA8)
2	SAOUHSC_01606	(Q2FY59_Q2FY59_STAA8)
2	SAOUHSC_01486	(Q2FYG6_Q2FYG6_STAA8)
2	SAOUHSC_01249	(Q2G2Q2_Q2G2Q2_STAA8)
2	SAOUHSC_01199	(Q2FZ53_Q2FZ53_STAA8)
2	SAOUHSC_01184	(Q2FZ67_Q2FZ67_STAA8)
2	SAOUHSC_01054	(Q2G2G7_Y1054_STAA8)
2	SAOUHSC_01014	(Q2FZI9_Q2FZI9_STAA8)
2	SAOUHSC_00834	(Q2G000_Q2G000_STAA8)
2	SAOUHSC_00794	(Q2G033_Q2G033_STAA8)
2	SAOUHSC_00508	(Q2G242_Q2G242_STAA8)
2	SAOUHSC_00442	(Q2G0T5_Q2G0T5_STAA8)
1	yajC	(Q2FXT7_Q2FXT7_STAA8)
1	secDF	(Q2FXT8_Q2FXT8_STAA8)
1	scaH	(Q2G222_Y2979_STAA8)
1	murl	(Q2FZC6_MURI_STAA8)
1	msrR	(Q7BHL7_MSRR_STAA8)

1	msrB	(POA088_MSRB_STAA8)
1	xerD	(Q2FY74_Q2FY74_STAA8)
1	uvrC	(Q2FZD0_UVRC_STAA8)
1	uvrA	(Q2G046_Q2G046_STAA8)
1	ugtP	(Q2FZP7_UGTP_STAA8)
1	tagX	(O05154_TAGX_STAA8)
1	srrB	(Q2FY80_SRRB_STAA8)
1	sarZ	(Q2FVN3_SARZ_STAA8)
1	sarS	(Q2G1N7_SARS_STAA8)
1	sarR	(Q9F0R1_SARR_STAA8)
1	sarA	(Q2G2U9_SARA_STAA8)
1	gdpp	(Q2G2T6_Q2G2T6_STAA8)
1	ruvB	(Q2FXT4_RUVB_STAA8)
1	rpsL	(POAOHO_RS12_STAA8)
1	rpsD	(Q2FXK6_RS4_STAA8)
1	rpml	(Q2FXQ0_RL35_STAA8)
1	rplW	(Q2FW08_RL23_STAA8)
1	rplP	(Q2FW13_RL16_STAA8)
1	rplN	(Q2FW16_RL14_STAA8)
1	rot	(Q9RFJ6_ROT_STAA8)
1	rnr	(Q2G024_Q2G024_STAA8)
1	recG	(O50581_RECG_STAA8)
1	pyrF	(Q2FZ71_PYRF_STAA8)
1	putP	(Q2FWY7_PUTP_STAA8)
1	nusG	(Q2G0P2_NUSG_STAA8)
1	mutS2	(Q2FZD3_MUTS2_STAA8)
1	mqo	(Q2FVQ5_Q2FVQ5_STAA8)
1	moaA	(P69848_MOAA_STAA8)
1	infC	(Q2FXP9_IF3_STAA8)

1	hslO	(Q2G0Q9_HSLO_STAA8)
1	hemH	(Q2FXA4_Q2FXA4_STAA8)
1	guaC	(Q2FYU4_GUAC_STAA8)
1	gmk	(Q2G1U0_KGUA_STAA8)
1	ftsY	(Q2FZ48_Q2FZ48_STAA8)
1	dltC	(Q2FZW4_DLTC_STAA8)
1	dinG	(Q2FYH5_DING_STAA8)
1	cvfB	(Q2FYP3_CVFB_STAA8)
1	сорА	(Q2FV64_COPA_STAA8)
1	cinA	(Q2FZ10_Q2FZ10_STAA8)
1	bioA	(Q2FVJ6_BIOA_STAA8)
1	atpF	(Q2G2F8_ATPF_STAA8)
1	addA	(Q2FZT5_ADDA_STAA8)
1	SAOUHSC_02525 (RND2)	(Q2FVZ5_Q2FVZ5_STAA8)
1	SAOUHSC_03016	(Q2FUT5_Q2FUT5_STAA8)
1	SAOUHSC_02971	(Q2FUX4_Q2FUX4_STAA8)
1	SAOUHSC_02956	(Q2FUY9_Q2FUY9_STAA8)
1	SAOUHSC_02947	(Q2FUZ8_Q2FUZ8_STAA8)
1	SAOUHSC_02791	(Q2FVC2_Q2FVC2_STAA8)
1	SAOUHSC_02760	(Q2FVF4_Q2FVF4_STAA8)
1	SAOUHSC_02727	(Q2FVI3_Q2FVI3_STAA8)
1	SAOUHSC_02723	(Q2FVI7_Q2FVI7_STAA8)
1	SAOUHSC_02690	(Q2G1U8_Q2G1U8_STAA8)
1	SAOUHSC_02681	(Q2FVM1_Q2FVM1_STAA8)
1	SAOUHSC_02668	(Q2FVN4_Q2FVN4_STAA8)
1	SAOUHSC_02660	(Q2FVP2_Q2FVP2_STAA8)
1	SAOUHSC_02649	(Q2FVQ3_Q2FVQ3_STAA8)
1	SAOUHSC_02648	(Q2FVQ4_Q2FVQ4_STAA8)
1	SAOUHSC_02629	(Q2G2W1_Q2G2W1_STAA8)

1	SAOUHSC_02614	(Q2FVS7_Q2FVS7_STAA8)
1	SAOUHSC_02601	(Q2FVU1_Q2FVU1_STAA8)
1	SAOUHSC_02583	(Q2FVV8_Q2FVV8_STAA8)
1	SAOUHSC_02555	(Q2FVW8_Q2FVW8_STAA8)
1	SAOUHSC_02554	(Q2FVW9_Q2FVW9_STAA8)
1	SAOUHSC_02553	(Q2FVX0_Q2FVX0_STAA8)
1	SAOUHSC_02544	(Q2FVX8_Q2FVX8_STAA8)
1	SAOUHSC_02406	(Q2FW93_Q2FW93_STAA8)
1	SAOUHSC_02381	(Q2FWB7_Q2FWB7_STAA8)
1	SAOUHSC_02374	(Q2FWC4_Q2FWC4_STAA8)
1	SAOUHSC_02357	(Q2FWE2_Q2FWE2_STAA8)
1	SAOUHSC_02352	(Q2G2F5_Q2G2F5_STAA8)
1	SAOUHSC_02197	(Q2FWT3_Q2FWT3_STAA8)
1	SAOUHSC_02161	(Q2FWW1_Q2FWW1_STAA8)
1	SAOUHSC_02098	(Q2FX09_Q2FX09_STAA8)
1	SAOUHSC_01987	(Q2FX90_Q2FX90_STAA8)
1	SAOUHSC_01979	(Q2FX98_Q2FX98_STAA8)
1	SAOUHSC_01978	(Q2FX99_Y1978_STAA8)
1	SAOUHSC_01977	(Q2FXA0_Y1977_STAA8)
1	SAOUHSC_01969	(Q2G2T0_Q2G2T0_STAA8)
1	SAOUHSC_01966	(Q2G2F2_Q2G2F2_STAA8)
1	SAOUHSC_01915	(Q2G2V2_Q2G2V2_STAA8)
1	SAOUHSC_01877	(Q2FXH0_Q2FXH0_STAA8)
1	SAOUHSC_01869	(Q2FXH8_Q2FXH8_STAA8)
1	SAOUHSC_01867	(Q2FXI0_Q2FXI0_STAA8)
1	SAOUHSC_01846	(Q2G294_Q2G294_STAA8)
1	SAOUHSC_01825	(Q2FXL0_Q2FXL0_STAA8)
1	SAOUHSC_01812	(Q2FXM3_Q2FXM3_STAA8)
1	SAOUHSC_01803	(Q2FXN2_Q2FXN2_STAA8)

1	SAOUHSC_01801	(Q2FXN4_Q2FXN4_STAA8)
1	SAOUHSC_01744	(Q2FXT9_Q2FXT9_STAA8)
1	SAOUHSC_01734	(Q2FXU8_Q2FXU8_STAA8)
1	SAOUHSC_01732	(Q2FXV0_Q2FXV0_STAA8)
1	SAOUHSC_01700	(Q2FXY0_Q2FXY0_STAA8)
1	SAOUHSC_01664	(Q2FY10_PDRP_STAA8)
1	SAOUHSC_01659	(Q2FY15_Q2FY15_STAA8)
1	SAOUHSC_01652	(Q2FY21_Q2FY21_STAA8)
1	SAOUHSC_01610	(Q2FY55_Y1610_STAA8)
1	SAOUHSC_01587	(Q2FY78_Q2FY78_STAA8)
1	SAOUHSC_01488	(Q2FYG4_Q2FYG4_STAA8)
1	SAOUHSC_01487	(Q2FYG5_Q2FYG5_STAA8)
1	SAOUHSC_01480	(Q2FYH2_Q2FYH2_STAA8)
1	SAOUHSC_01455	(Q2FYJ0_Q2FYJ0_STAA8)
1	SAOUHSC_01436	(Q2FYK4_Y1436_STAA8)
1	SAOUHSC_01284	(Q2FYY8_Q2FYY8_STAA8)
1	SAOUHSC_01279	(Q2FYZ3_Q2FYZ3_STAA8)
1	SAOUHSC_01267	(Q2FZ04_Q2FZ04_STAA8)
1	SAOUHSC_01258	(Q2FZ13_Q2FZ13_STAA8)
1	SAOUHSC_01214	(Q2FZ39_Q2FZ39_STAA8)
1	SAOUHSC_01198	(Q2FZ54_Q2FZ54_STAA8)
1	SAOUHSC_01179	(Q2G266_Q2G266_STAA8)
1	SAOUHSC_01031	(Q2FZH3_Q2FZH3_STAA8)
1	SAOUHSC_01016	(Q2FZI7_Q2FZI7_STAA8)
1	SAOUHSC_00989	(Q2FZL1_Q2FZL1_STAA8)
1	SAOUHSC_00982	(Q2FZL8_Q2FZL8_STAA8)
1	SAOUHSC_00974	(Q2FZM6_Q2FZM6_STAA8)
1	SAOUHSC_00951	(Q2FZP9_Y951_STAA8)
1	SAOUHSC_00946	(Q2FZQ4_Q2FZQ4_STAA8)

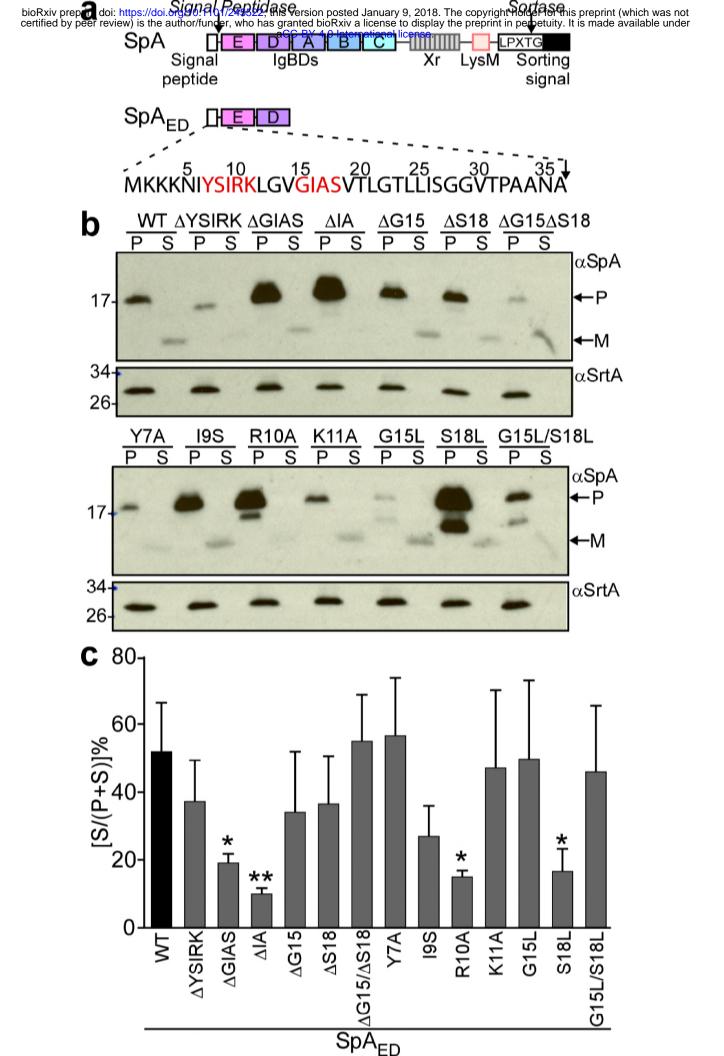
1	SAOUHSC_00925	(Q2FZR5_Q2FZR5_STAA8)
1	SAOUHSC_00909	(Q2FZT1_Q2FZT1_STAA8)
1	SAOUHSC_00897	(Q2FZU3_Q2FZU3_STAA8)
1	SAOUHSC_00873	(Q2FZW2_Q2FZW2_STAA8)
1	SAOUHSC_00855	(Q2FZX9_2NPD_STAA8)
1	SAOUHSC_00847	(Q2FZY7_Q2FZY7_STAA8)
1	SAOUHSC_00792	(Q2G035_Y792_STAA8)
1	SAOUHSC_00730	(Q2G090_Q2G090_STAA8)
1	SAOUHSC_00727	(Q2G094_Q2G094_STAA8)
1	SAOUHSC_00711	(Q2G2T9_Q2G2T9_STAA8)
1	SAOUHSC_00707	(Q2G238_Q2G238_STAA8)
1	SAOUHSC_00640	(Q2G2L3_Q2G2L3_STAA8)
1	SAOUHSC_00639	(Q2G2K9_Q2G2K9_STAA8)
1	SAOUHSC_00547	(Q2G0L3_Q2G0L3_STAA8)
1	SAOUHSC_00483	(Q2G0R3_Q2G0R3_STAA8)
1	SAOUHSC_00444	(Q2G0T4_Y444_STAA8)
1	SAOUHSC_00413	(Q2G0W1_Y413_STAA8)
1	SAOUHSC_00398	(Q2G0X5_Q2G0X5_STAA8)
1	SAOUHSC_00333	(Q2G1V4_Q2G1V4_STAA8)
1	SAOUHSC_00307	(Q2G148_Q2G148_STAA8)
1	SAOUHSC_00269	(Q2G178_Q2G178_STAA8)
1	SAOUHSC_00268	(Q2G179_Q2G179_STAA8)
1	SAOUHSC_00261	(Q2G185_Q2G185_STAA8)
1	SAOUHSC_00236	(Q2G1A9_Q2G1A9_STAA8)
1	SAOUHSC_00196	(Q2G1C9_Q2G1C9_STAA8)
1	SAOUHSC_00126	(Q2G1J6_Q2G1J6_STAA8)
1	SAOUHSC_00039	(Q2G1R3_Q2G1R3_STAA8)

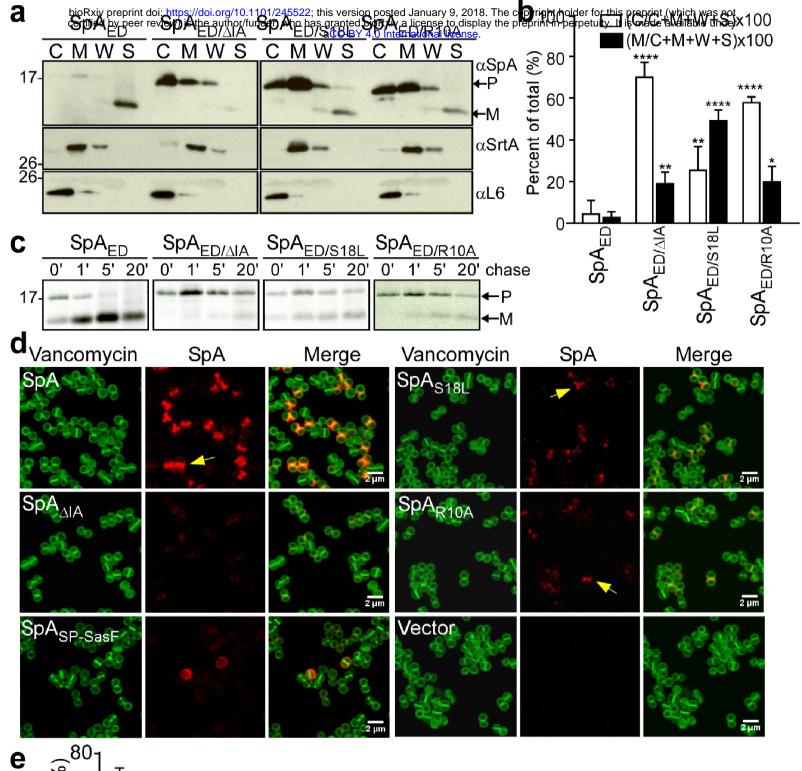
Strain or plasmid	Description	Reference or source		
E. coli DC10B	Cloning strain	(Monk et al., 2012)		
<i>E. coli</i> DH5α	Cloning strain	(Hanahan, 1983)		
<i>S. aureus</i> RN4220	S. aureus laboratory strain	(Kreiswirth et al., 1983)		
<i>S. aureus</i> SEJ1	Δ <i>spa</i> in RN4220	(Gründling and		
		Schneewind, 2007)		
S. aureus WY110	Δspa Δsbi, sbi::ermB in S. aureus SEJ1	This work		
S. aureus WY223	P _{spac} -secA in S. aureus RN4220	This work		
S. aureus WY230	P _{tet} -secA:sfGFP in S. aureus WY223	This work		
<i>S. aureus</i> ANG499	P _{spac} -ItaS in S. aureus RN4220	(Gründling and		
		Schneewind, 2007)		
S. aureus WY418	ΔsecDF in S. aureus RN4220	This work		
S. aureus WY416	Δ <i>rnd2</i> in <i>S. aureus</i> RN4220	This work		
<i>S. aureus</i> WY400	Δ <i>rnd3</i> in <i>S. aureus</i> RN4220	This work		
S. aureus WY412	$\Delta secDF \Delta rnd2\Delta rnd3$ in <i>S. aureus</i> RN4220	This work		
pOS1	E. coli/S. aureus shuttle vector	(Schneewind et al., 1993		
pSpA _{ED}	spa promoter, signal peptide and IgBDs E	This work		
	and D in pOS1			
pSpA _{ED/R10A}	R10A variant of pSpA _{ED}	This work		
pSpA _{ED/S18L}	S18L variant of of $pSpA_{ED}$	This work		
pSpA _{ED/ΔIA}	ΔIA variant of $pSpA_{ED}$	This work		
pCL55	S. aureus integration vector	(Lee et al., 1991)		
pCL55-SpA	Full length spa with its native promoter	This work		
	cloned in pCL55			
pCL55-SpA _{R10A}	R10A variant of pCL55-SpA	This work		
pCL55-SpA _{S18L}	S18L variant of pCL55-SpA	This work		
pCL55-SpA $_{\Delta IA}$	ΔIA variant of pCL55-SpA	This work		
pCL55-SpA _{SP-SasF}	SpA signal peptide replaced by SasF signal	This work		
	peptide in pCL55-SpA			
pCL55-P _{tet}	pCL55 with anhydro-tetracycline inducible	(Gründling and		

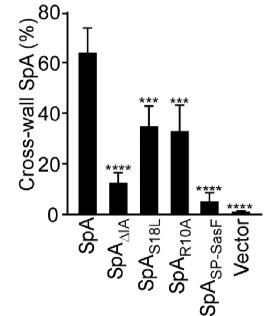
	promoter	Schneewind, 2007)
pCL55-P _{tet} -	SecA-sfGFP hybrid cloned into pCL55- P_{tet}	This work
secA:sfGFP		
pMutin–HA	Single copy integration vector	Bacillus Genetic Stock
		Center
pMutin–HA-5'secA	secA promoter and 656 bp in pMutin-HA	This work
pKOR1-secDF	allelic replacement vector for secDF1	This work
	deletion	
pKOR1-rnd2	allelic replacement vector for secDF2	This work
	deletion	
pSecDF	secDF ORF and 274 bp upstream in pOS1	This work

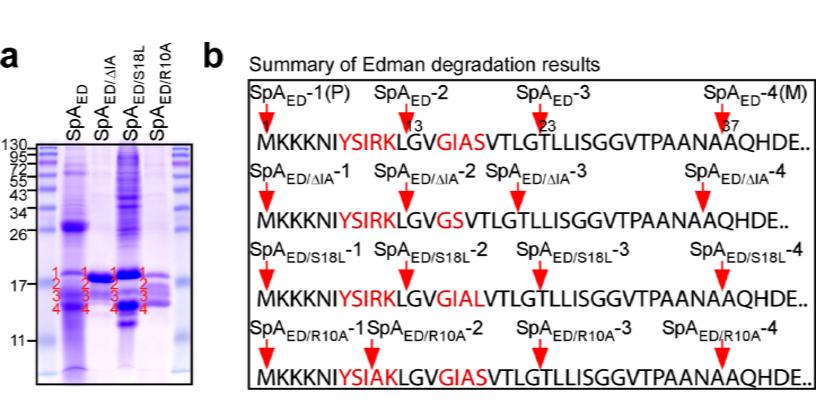
Primer	^a Direction	Sequence	Plasmid
10	F	GCGTAGTATTGCAATACATAATTCGTTA	pSpA _{ED}
69	R	TTTTGGATCCTTACATTTTCGGTGCTTGAGATTCGTT	pSpA _{ED}
38	R	TGCAATACCTACACCTAGAATGTTTTTCTTTTTCA	pSpA _{ed/aysirk}
39	F	GAAAAAGAAAAACATTCTAGGTGTAGGTATTGCATC	pSpA _{ed/aysirk}
49	R	TGTACCTAAAGTTACTACACCTAGTTTACGA	pSpA _{ED/ΔGIAS}
50	F	TCGTAAACTAGGTGTAGTAACTTTAGGTACA	pSpA _{ED/ΔGIAS}
51	R	TGTACCTAAAGTTACTGCAATTACACCTAGT	pSpA _{ed/ag15as18}
52	F	ACTAGGTGTAATTGCAGTAACTTTAGGTACA	pSpA _{ed/ag15as18}
53	R	ACCTAAAGTTACAGAACCTACACCTAGTTTAC	pSpA _{ED/ΔΙΑ}
54	F	GTAAACTAGGTGTAGGTTCTGTAACTTTAGGT	pSpA _{ED/ΔΙΑ}
55	R	AGTTACAGATGCAATTAATACACCTAGTTTACGA	pSpA _{ED/G15L}
56	F	TCGTAAACTAGGTGTATTAATTGCATCTGTAACT	pSpA _{ED/G15L}
57	R	TGTACCTAAAGTTACTAATGCAATACCTACACCT	pSpA _{ED/S18L}
58	F	AGGTGTAGGTATTGCATTAGTAACTTTAGGTACA	pSpA _{ED/S18L}
70	R	AGTAATGTACCTAAAGTTACCAATGCAATTAATACACCTAGT	pSpA _{ED/G15L/S18L}
71	F	ACTAGGTGTATTAATTGCATTGGTAACTTTAGGTACATTACT	pSpA _{ED/G15L/S18L}
72	R	AGTAATGTACCTAAAGTTACAGATGCAATTACACCTAGTTTACGA	$pSpA_{ED/\Delta G15}$
73	F	TCGTAAACTAGGTGTAATTGCATCTGTAACTTTAGGTACATTACT	$pSpA_{ED/\Delta G15}$
74	R	ACCTAAAGTTACTGCAATACCTACACCTAGTTTACGAATTGA	$pSpA_{ED/\Delta S18}$
75	F	TCAATTCGTAAACTAGGTGTAGGTATTGCAGTAACTTTAGGT	$pSpA_{ED/\Delta S18}$
84	R	ATACCTACACCTAGTTTAGCAATTGAATAAATGTTT	pSpA _{ED/R10A}
85	F	AAACATTTATTCAATTGCTAAACTAGGTGTAGGTAT	pSpA _{ED/R10A}
92	R	TAGTTTACGAATTGAAGCAATGTTTTCTTTTCA	pSpA _{ED/Y7A}
93	F	TGAAAAAGAAAAACATTGCTTCAATTCGTAAACTA	pSpA _{ED/Y7A}
94	R	TACACCTAGTTTACGAGATGAATAAATGTTTTTCT	pSpA _{ED/I9S}
95	F	AGAAAAACATTTATTCATCTCGTAAACTAGGTGTA	pSpA _{ED/I9S}
96	R	TGCAATACCTACACCTAGAGCACGAATTGAATAAATGT	pSpA _{ED/K11A}
97	F	ACATTTATTCAATTCGTGCTCTAGGTGTAGGTATTGCA	pSpA _{ED/K11A}
175	F	GCGGGATCCTAGTATTGCAATACATAATTCGTTA	pCL55-SpA
177	R	GCGGGTACCTTATAGTTCGCGACGACGTCCAGCT	pCL55-SpA
21	R	ATTAATACCCCCTGTATGTATTTGT	pCL55-SpA _{SP-Sa}
22	F	TACAGGGGGTATTAATATGGCTAAATATCGAGGGAAAC	pCL55-SpA _{SP-Sat}

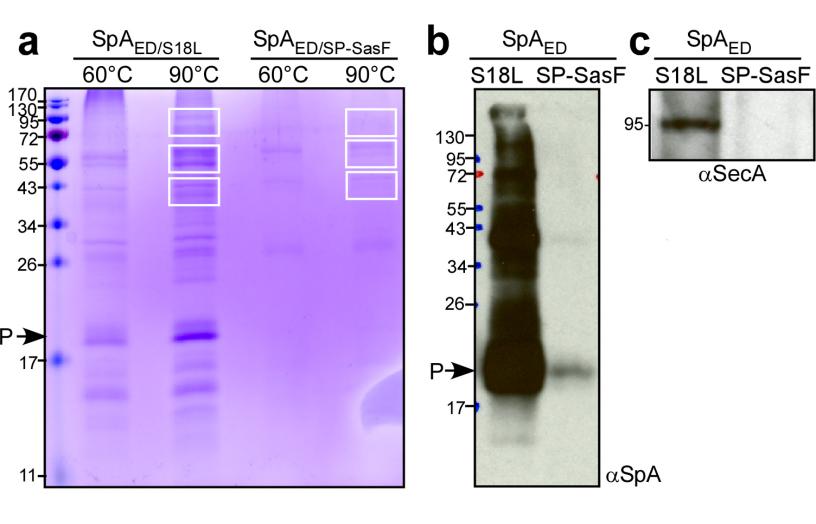
23	R	TGTTGAGCTTCATCGTGTTGCGCAGCTTGGGCATCGTACGGCAAGA	pCL55-SpA _{SP-SasF}		
24	F	GCGCAACACGATGAAGCTCAACAA	pCL55-SpA _{SP-SasF}		
189	F	CCCAAGCTTTAGCTAAAGGAGCGAACGAAATGGGA	pMUTIN-HA-5' <i>secA</i>		
190	R	GCGGGTACCTGAGTCAACCTCATCAATGATTGCA	pMUTIN-HA-5' <i>secA</i>		
180	F	CTCCCTAGGTAAAGGAGCGAACGAAATGGGAT	pCL55-P _{tet-}		
			secA:sfGFP		
181	R	TGCAGCTCCTGCGGCGCCTCCTTTTCCATGGCAATTTTTGA	pCL55-P _{tet-}		
			secA:sfGFP		
182	F	AGGAGGCGCCGCAGGAGCTGCATCAAAAGGTGAAGAATT	pCL55-P _{tet-}		
			secA:sfGFP		
183	R	CTCAGATCTTTATTATAATTCATCCATACCA	pCL55-P _{tet-}		
			secA:sfGFP		
295	F	GGGGACAAGTTTGTACAAAAAAGCAGGCTAATATTGTCATTGTATCCCGCTTCT	pKOR1- <i>secDF</i>		
313	R	ACATACGTAAATATCGAACGATGAAAAGATTTTAGT	pKOR1- <i>secDF</i>		
314	F	TCATCGTTCGATATTTACGTATGTATTTAGAATACT	pKOR1- <i>secDF</i>		
298	R	GGGGACCACTTTGTACAAGAAAGCTGGGTTGAACATACAGAGCAGTTTATGCCT	pKOR1-secDF		
305	F	GGGGACAAGTTTGTACAAAAAAGCAGGCTACATACTCCACAGATATTTTAGA	pKOR1-rnd2		
306	R	TGAATATAGATAATATAAAAGCCATAAAAGCGGT	pKOR1-rnd2		
307	F	TGGCTTTTATATTATCTATATTCAAAAATATTTTACT	pKOR1-rnd2		
308	R	GGGGACCACTTTGTACAAGAAAGCTGGGTTCGATCCTGATGTTGAAGTTGAT	pKOR1-rnd2		
315	F	GCGGAATTCTGAGAAGTGGTATTAAAAAGGATGA	pSecDF		
316	R	GCGGGATCCTTAAACTAAAATCTTTTCATCGTTCGA	pSecDF		
^a PCR pri	^a PCR primer direction for forward (F) or reverse (R) amplification of template DNA.				

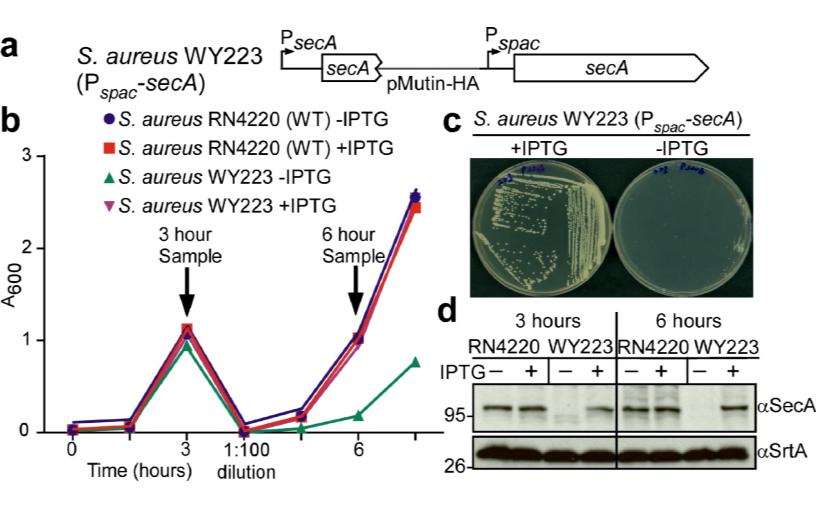


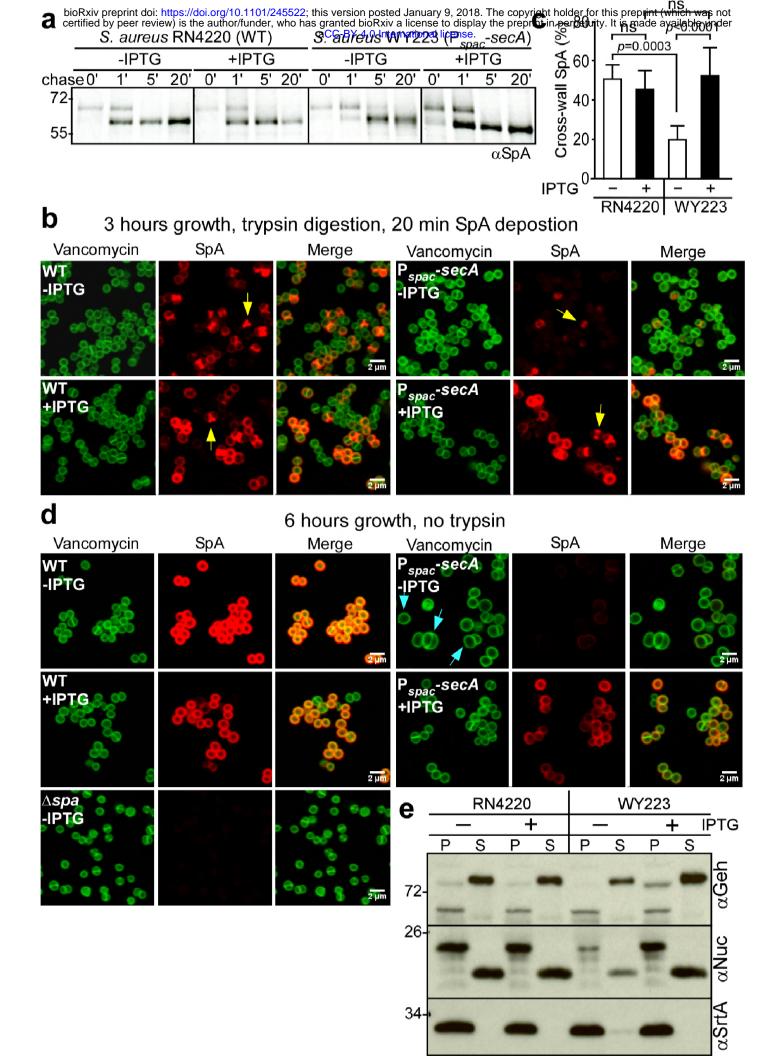


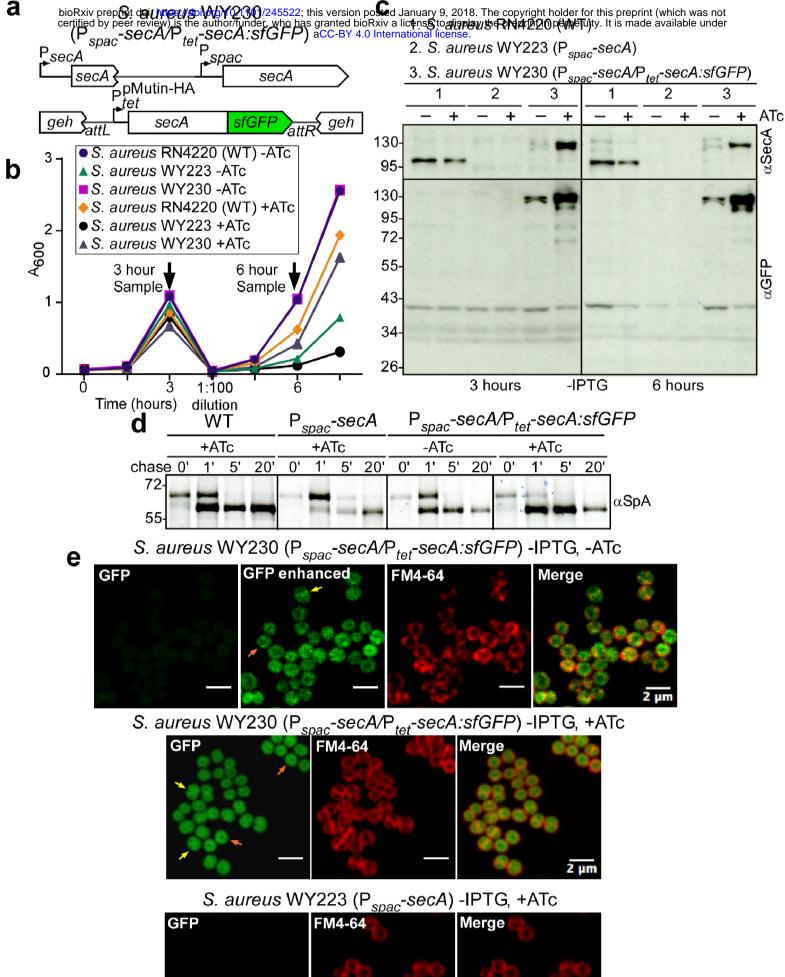




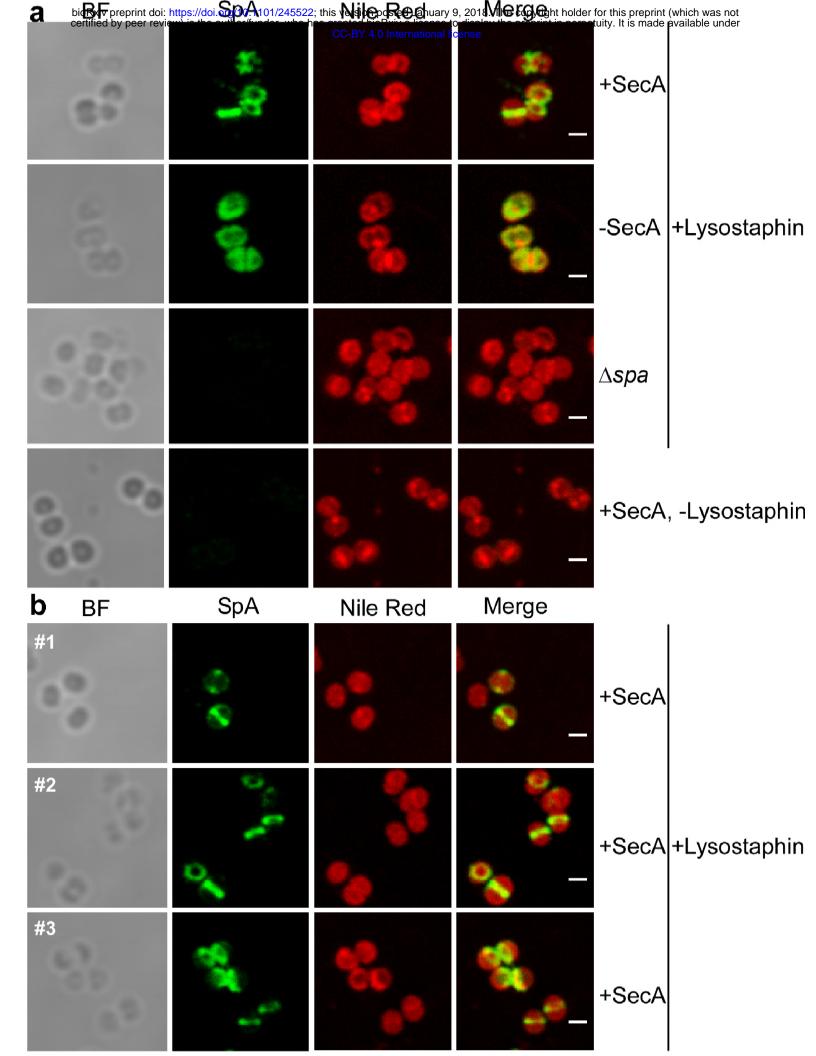


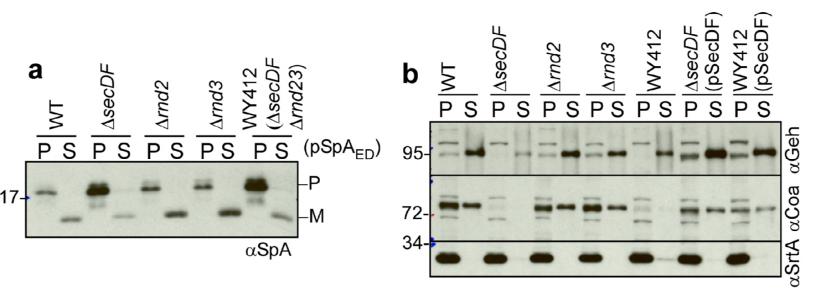






2 µm





С	SpA	Nile Red	Merge	BF	SpA	Nile Red	Merge	BF
V	/T(pOS1)	E.F	50° 0.		∆rnd3	*	* *-	8° 8
∆ (r	secDF IOS1)	-		4 (B) (B)	WY412 (pOS1)	2.90 2.90		23°
∆ (r	secDF SecDF)		**	24 09	WY412 (pSecDF)	48 8	*	45
Δ	rnd2	. 3	*	90	∆spa	₩2 ₩2 ₩2	۲ <mark>او</mark> د نو	10 10 m

